A Road Map toward Field-Effect Transistor Biosensor Technology for Early Stage Cancer Detection

small methods
www.small-methods.com

A Road Map toward Field-Effect Transistor Biosensor Technology for Early Stage Cancer Detection

*Muthusankar Eswaran, Bavatharani Chokkiah, Santosh Pandit, Shadi Rahimi, Ragupathy Dhanusuraman, Mahaboobbatcha Aleem, and Ivan Mijakovic**

Field effect transistor (FET)-based nanoelectronic biosensor devices provide a viable route for specific and sensitive detection of cancer biomarkers, which can be used for early stage cancer detection, monitoring the progress of the disease, and evaluating the effectiveness of therapies. On the road to implementation of FET-based devices in cancer diagnostics, several key issues need to be addressed: sensitivity, selectivity, operational conditions, anti-interference, reusability, reproducibility, disposability, large-scale production, and economic viability. To address these well-known issues, significant research efforts have been made recently. An overview of these efforts is provided here, highlighting the approaches and strategies presently engaged at each developmental stage, from the design and fabrication of devices to performance evaluation and data analysis. Specifically, this review discusses the multistep fabrication of FETs, choice of bioreceptors for relevant biomarkers, operational conditions, measurement configuration, and outlines strategies to improve the sensing performance and reach the level required for clinical applications. Finally, this review outlines the expected progress to the future generation of FET-based diagnostic devices and discusses their potential for detection of cancer biomarkers as well as biomarkers of other noncommunicable and communicable diseases.

1. Introduction

Cancer is one of the leading causes of mortality worldwide and represents a serious and complex healthcare problem. With the ageing world population, the prevalence of cancer is expected to increase. Cancer is a complex and variable disease, based on a unique pattern of mutations accumulated in each patient, hence requiring individual approaches of personalized/precision medicine. Accurate diagnostics, powerful enough to ensure early detection, is the key to the survival of cancer patients.[1–6] Cancer biomarkers (encompassing metabolites, peptides/proteins, and nucleic acids-based markers) play a vital role in detecting cancers and monitoring their progression as well as in evaluating treatment effectiveness. Even minor changes in the levels of cancer biomarkers are very relevant for diagnostics. These minor changes need to be detected in complex biological samples, such as blood, saliva, urine, and/or other body fluids.[7–12] Hence, ultrasensitive and very specific diagnostic tools are required for the detection and quantification of such biomarkers. Conventional cancer detection methods such as computed tomography, cytological detection, magnetic resonance imaging, fluorescence imaging, immunohistochemistry, thermography, X-ray technique, radioimmunoassay, enzyme-linked immunosorbent assay (ELISA), and ultrasound method, typically encompass several stages, e.g., complex pretreatment processes, time-consuming nucleic acid amplification or mass spectrometry analysis of protein biomarkers. In addition to being time-consuming, existing diagnostic tools are also typically expensive, and in some cases lack the required sensitivity and specificity, which limits their utility in clinical diagnostics.[13–16] Recent advancements in micro/nanoelectromechanical system (M/NEMS) technology show their potential to overcome such drawbacks and have the possibility to fabricate a miniaturized device with highly selective and sensitive clinical diagnostic functions.

M. Eswaran, S. Pandit, S. Rahimi, I. Mijakovic
Division of Systems and Synthetic Biology
Department of Biology and Biological Engineering
Chalmers University of Technology
41296 Göteborg, Sweden
E-mail: ivan.mijakovic@chalmers.se

The ORCID identification number(s) for the author(s) of this article can be found under https://doi.org/10.1002/smtd.202200809.

DOI: 10.1002/smtd.202200809

B. Chokkiah, R. Dhanusuraman
Nanoelectrochemistry Lab
Department of Chemistry
National Institute of Technology Puducherry
Karaikal 609609, India

M. Aleem
Department of Electrical Engineering
City College of New York
New York 10031, USA

I. Mijakovic
Novo Nordisk Foundation Center for Biosustainability
Technical University of Denmark
2800 Lyngby, Denmark

Such miniaturized devices, based on the M/NEMS, are already recognized as being consistent, economical, ultrasensitive, and highly selective, and hence suitable for noninvasive early stage detection of cancer biomarkers in the body fluids.[17–22]

The biosensor devices based on M/NEMS technology act as transducers, which convert a biological/chemical response instigated by an explicit target analyte (or a group of analytes) into an assessable electrical signal, proportional to the concentration of the target analyte(s). To understand and fabricate a practical biosensor, two important parameters are essential. The first is a bioreceptor/biorecognition element (such as antibodies, enzymes, aptamers, and DNA). The second is a signal transduction unit, which translates the interaction between the biological/chemical analyte and bioreceptor element (input) into an assessable signal (output), which can be electrochemical, electrical, mechanical, optical, etc. The readout of the acquired signal typically requires some manipulation, which should preferably occur on the same unit as the detection.[23–31]

A field-effect transistor (FET)-based biosensor is one type of electrical biosensor that attracted much attention in the past decade, owing to its suitability for devices used for point-of-care diagnostics, as well as in other fields such as, e.g., monitoring of environmental pollution, food quality, and pharmaceuticals. FET devices directly translate the analyte-receptor interaction into electrical signals. Thus, the binding of analytes to receptors can be detected by tracking changes in the electrical conductivity or resistance of the FET channel. The basis for this is a transformation of the receptor molecule (oxidation/reduction or other types of conversion), triggered by the binding of the analyte. This transformation causes a change in the current and threshold voltage of the FET biosensor device.[32–35] The complete multistep fabrication process of FET biosensors is depicted in **Figure 1**. Based on the efficient and simple detection process, FET biosensors can be effectively utilized for the detection of noncommunicable and communicable diseases as shown in **Figure 2**.

In this review, recent trends in the FET biosensor development toward cancer detection are discussed, focusing on the basic working principles, materials and device fabrication, biomarkers, bioreceptors, factors that can improve the sensing performance, and current challenges and perspectives for this field.

2. FET Biosensor: Materials and Fabrication Techniques

In this section, the various materials and substrates used for the conductive metal contacts or electrodes (such as source, drain, and gate), metal oxide/electrolyte (dielectric), and a channel are discussed. Further, the fabrication techniques used to deposit/grow the materials to obtain source, drain, and gate electrodes on the substrate are discussed in this section.

2.1. Substrates for the FET Biosensor Device

The design and fabrication of a new device need to be strategic, guided by the specific application and by the characteristic of individual substrates. Devices can be flexible, portable, miniaturized, operated in specific conditions, requiring chemical stability, etc. to meet the demanding specifications of the realistic applications. In FET nanoelectronics, the Si-SiO_2 wafer is the preferred substrate, owing to its compatibility

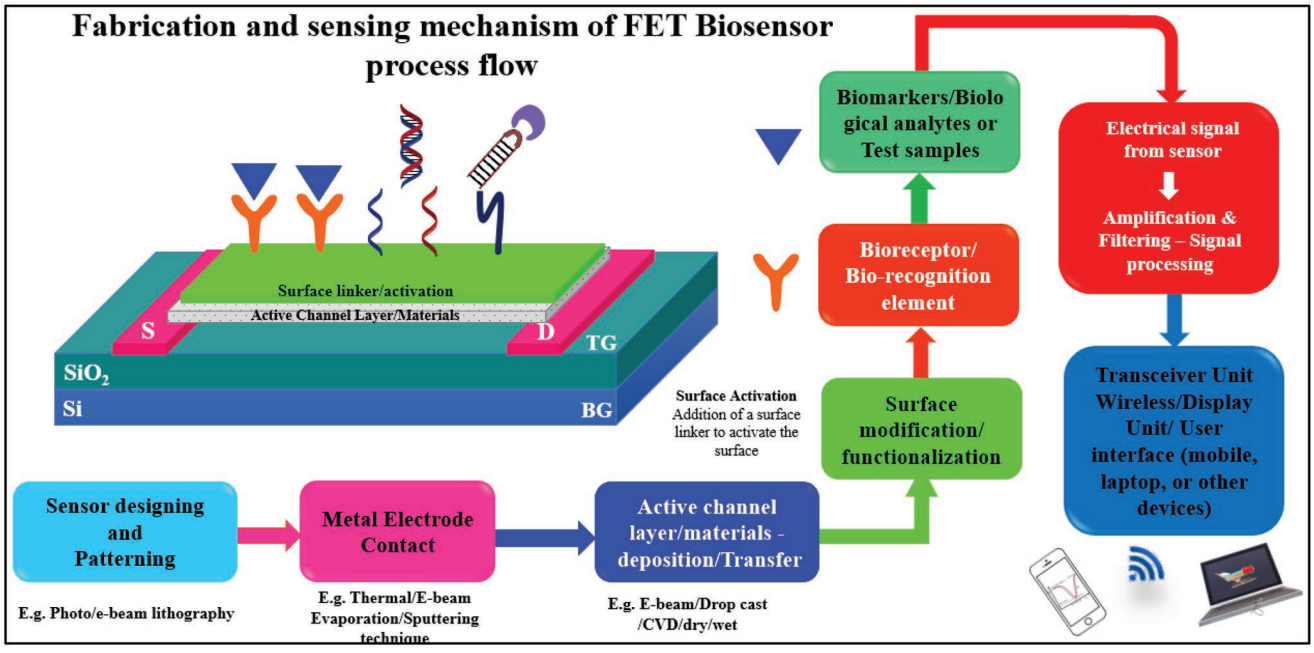

Figure 1. FET biosensor fabrication and sensing mechanism-process flow.

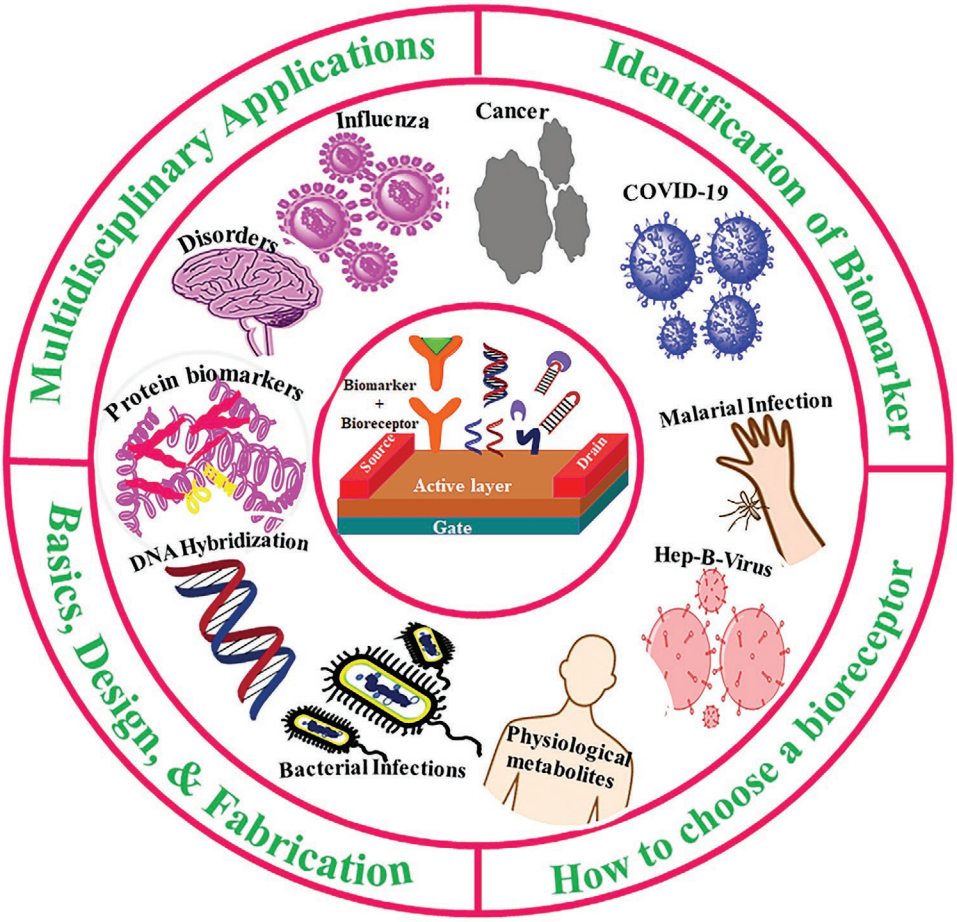

Figure 2. FET biosensor based highly sensitive clinical diagnostics applications.

with most operating conditions.[36–51] Some other typically used firm substrates include quartz[52,53] and glass.[54] On the other hand, the progress toward flexible, wearable devices mainly focus on the flexible substrates which fall into several categories: i) polymer plastic substrates: polyimide, (polyethylene terephthalate, polycarbonate, polyethylene naphthalate), ii) polymer elastomers: polydimethylsiloxane, polyurethane, thermoplastic polyurethane, styrene-ethylene/butylene-styrene, and iii) hydrogel and polymer foams.[58,61–68,73,74] Recently, the substrates employed were coated with different dielectric materials (such as aluminum oxide (Al_2O_3) and hafnium oxide (HfO_2)) to play with operating voltage, environmental conditions, etc. to optimize or improve the performance of the sensor.[57,58]

2.2. Source and Drain

The conductive materials with low contact resistance and good adhesion to substrates are usually the obvious choice for the source (S) and drain (D) electrodes in the fabrication process. Gold (Au) is typically used as the conductive electrode pad for the S and D terminal in most of the published work. To intensify its adhesion, chromium (Cr) and titanium (Ti) are used along with it. Palladium (Pd), nickel (Ni), copper (Cu), silver (Ag), aluminum (Al), and molybdenum (Mo), poly(3,4-ethylene dioxythiophene): polystyrene sulfonate (flexible substrates), etc. have also been used for the same purpose. The fabrication of S and D involves sophisticated instrumentations to deposit the metal contacts using electron-beam or thermal evaporation/deposition, sputtering,[38–48,50–52,55–68,73,74], etc.

2.3. Gate

The device is commonly biased with a gate voltage that produces the electric field effect that accelerates the concentrations of the charge carriers and the current between the S and D electrode pads. It is generally biased using a back gate or a top gate (mainly with a background electrolyte/solution-gated device). Back, top, and solution/electrolyte gated FET biosensors are schematically presented in **Figure 3**A–C.[54,57] Also, dual or double gate sensor devices were reported to improve the sensitivity however owing to their fabrication complexity shrinks its popularity. Thus, the usage of the back gate still grabs attention among the sensor research community which offers rapid response kinetics and simple fabrication steps.[58]

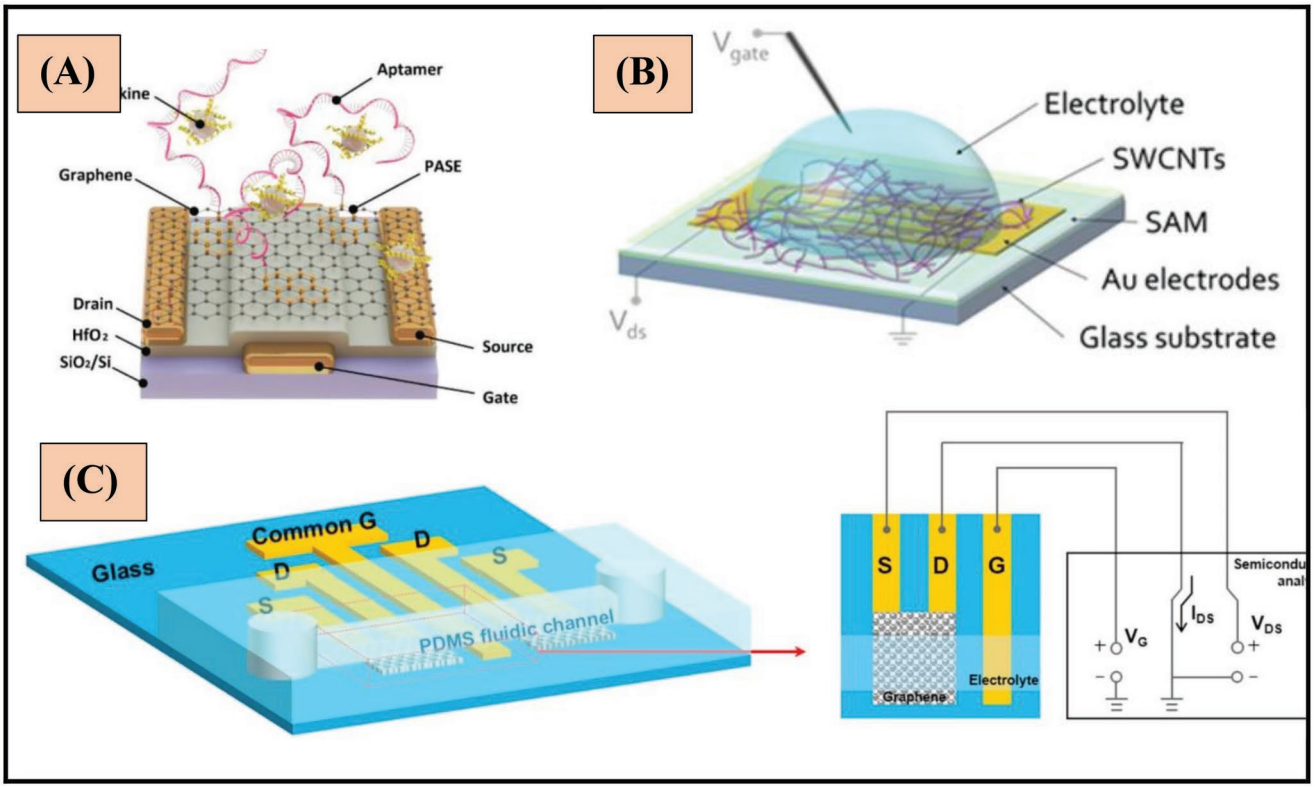

Figure 3. A) Back gate. Reproduced with permission.[57] Copyright 2019, Elsevier. B) Top gate. Reproduced with permission.[54] Copyright 2019, American Chemical Society. C) Solution gate FET biosensor. Reproduced with permission.[83] Copyright 2017, Elsevier.

3. FET Biosensor: Structure, Working Principle, and Configurations

3.1. Structure of FET Biosensor

The usual structure of an FET biosensor is schematically presented along with its multistep fabrication and operation in Figure 1. The sensor operation is based on an active channel layer, which was systematically deposited on a dielectric substrate (Si/SiO_2 layer-based wafer is commonly utilized for this). The active channel layer/material(s) (e.g., graphene) is surface-functionalized/activated using a bioreceptor/recognition element to capture or sense the analyte of interest. Then, a back gate or a top gate bias system typically gets engaged to evaluate the sensing performance of the functionalized FET device.

3.2. Surface Functionalization/Immobilization of a Bioreceptor on the Active Layer

Surface functionalization or immobilization is a process of attaching biological receptors on the top or inside a matrix/support. This attachment can be chemical or physical, and it allows receptor transformation upon binding the analyte, to be conveyed to the sensor. The process of immobilization can be achieved by direct or indirect techniques, resulting in coupling the bioreceptors to the active layer.

The direct approach employs covalent linkage, whereby the bioreceptor is directly and covalently attached to the active layer surface of an FET device, using chemical or physical approaches. Many categories of bioreceptors, such as purified proteins (purity level greater than 50%), can be immobilized using this approach. However, the invasive and irreversible nature of this approach (covalent bonds) often results in reduced affinity of the receptor toward the target bioanalytes and it limits sensor surface reusability. In the indirect approach of immobilization, first the target molecule is fixed to the carrier and then covalently coupled to the sensor's surface. The direct usage of impurified target molecules offers insignificant heterogeneous affinity and facilitates in reusability of the sensor surface, making this approach better and more widely employed than the direct coupling method. As mentioned above, the generally used functionalization/immobilization approaches can be chemical or physical. The binding of biological receptors can be done simply by adsorption to the active layer of the sensor surface in a physical approach shown in **Figure 4**Aa. The physical approach involves a conformational change via weak and noncovalent binding or deposition forces including electrostatic, van der Waal's interactions, and hydrogen bonding interactions between the sensor surface and the target analyte. Owing to their weak and noncovalent interactions, the dependencies (temperature, pH, concentration, and ionic strength), performance, stability, and reusability of the sensor are heavily affected, thus depriving its attention extensively.[68–75]

The chemical approaches answer the above deficiencies to achieve effective sensor performance by covalent, crosslinking, and bioconjugation affinity (BA) of the target molecules.

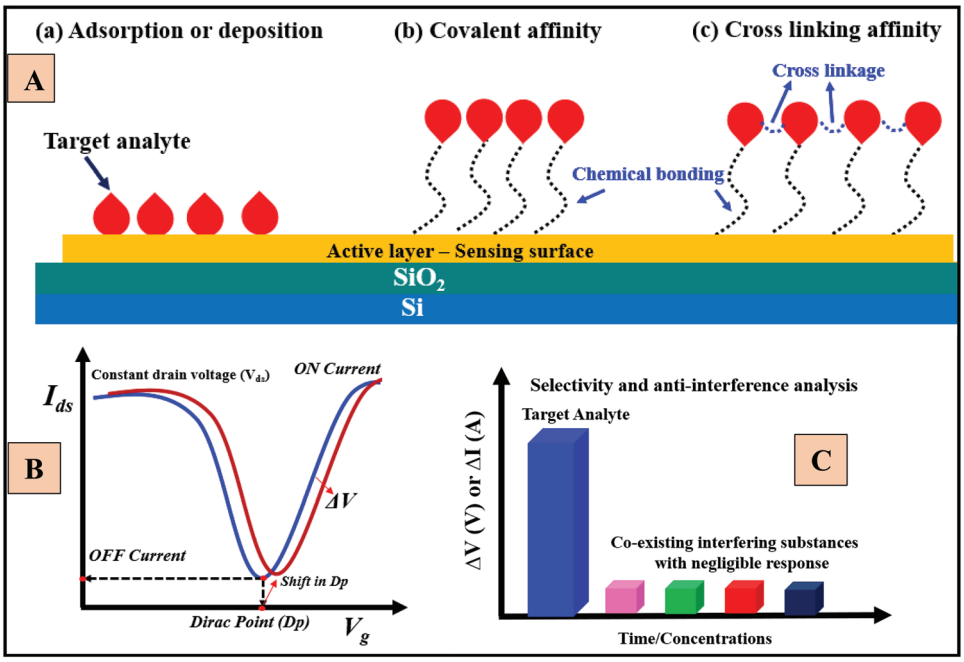

Figure 4. A) Surface functionalization/immobilization: a) adsorption or deposition, b) covalent affinity, and c) crosslinking affinity. B) Measurement of drain–source current versus gate voltage, and C) selectivity and interference analysis.

i) Covalent affinity (CA): The formation of covalent bonds between the sensor surface and target molecule/analyte is depicted in Figure 4Ab. Covalent affinities are usually formed via a simple chemical reaction with surface-active functional groups existing on the active layer of the sensor surface. Owing to its stable and strong attachment, good ionic diffusion, nominal seepage of analyte, and long life span it attracts much attention. CA also holds some drawbacks, limiting its applicability in some cases due to its complexity, nonreusable functionalized surface, and uncontrolled biorecognition elements influencing the sensor performances.
ii) Crosslinking affinity (CLA): The crosslinkage forms a seized stable crosslinked aggregates and effectively captures the target analytes by engaging reagents/compounds with two or multiple active functional groups as depicted in Figure 4Ac. The involvement of reagents/compounds (if toxic) damages the active layer of the sensor surface.
iii) BA: a number of proteins–small molecule affinity and protein–protein interactions have been attached for immobilization over the active site. Owing to the selective interactions of proteins entrapment, the active site becomes highly target-specific and selective with superior sensitivity.

Also, some other approaches have been engaged to functionalize or attach the bioreceptors such as self-assembly monolayer and Langmuir–Blodgett film technology.[68–70,76–80]

3.3. Sensing Mechanism and Evaluation

After the functionalization/immobilization of the active layer of the FET sensor surface, the sensing performance can be evaluated by a back gate or a top gate bias system which is typically engaged. The bias applied creates the electric field effect that regulates the concentrations of the charge carrier and the current between the source and drain terminals (I_{ds}). By considering FET based graphene layer as the active channel, a familiar I_{ds}–V_g curve for a constant drain voltage (V_{ds}) is presented in Figure 4B.[27] Here as depicted, the critical transition voltage between the two areas is termed the Dirac point (D_p). The number of charge carriers in the active material/layer is nominal at the D_p and thus the current between the source and drain terminal is denoted as the "OFF" current (I_{OFF}). At the saturation current, the I_{ds} have no dependency on the V_g, which is denoted as the "ON" current (I_{ON}). Using this I_{ON} and I_{OFF} current ratio, the effect of sensitivity can also be investigated during the interaction between the bioreceptor and target analytes.

The biosensing of a target analyte using FET is achieved by applying a constant V_{ds} and V_g, and the I_{ds} can be measured with respect to the time at the constant environmental conditions (constant temperature, pH, chemicals ambiance, humidity, etc.). Typical bioanalytes include blood, serum, urine, saliva, and sweat, which are used directly for sensing or first get diluted in some buffer. These analytes are subjected to FET analysis by placing them over their electrically active channel. There is typically a period of time called stabilization/settling time, or sensing/detection time, during which the interaction between the biorecognition element (receptor) and the targeted bioanalyte(s) will lead to changes in the concentration of charge carriers of the electrically conducting channel. Subsequently, the change in the current and conductance will be measured using the following equation (the n-type charge concentration is assumed).

$$I = \frac{en\mu_n wt}{L}V \quad (1)$$

where e, n, and μ_n, w, t, and L, and V are the electron charge, concentration, and mobility of electron, width, thickness, length of the active channel, and voltage, respectively. As per Equation (1), changes in charge carrier concentration influence the current, but the current also depends on the mobility and channel dimensions. To achieve ultrasensitive performance, all the parameters including charge carrier concentration, mobility, and dimensions of the channel need to be as high as possible. The change in concentration of the charge carrier leads to the change or shift in Dirac voltage point (ΔV) as depicted in Figure 4B, which reveals the noticeable changes that arose owing to the interactions between the biorecognition element and target analyte during the evaluation of sensing performance of FET biosensor device.

3.4. Configuration of FET Device

The sensing performance mainly depends on the configuration of the FET biosensor device which is classified as back, top, and solution gate configurations.

i) Back-gate configuration: The back-gate configured FET biosensor has a maximum sensing zone as depicted in Figure 3A. A Si substrate is used as a common back gate and a SiO_2 as a gate dielectric layer of this kind of FET device. Cytokine biomarkers are detected using a back gate configuration using saliva in this work.[57]
ii) Top-gate configuration: The top-gate configured FET biosensor fabrication is relatively facile and it also exhibits significant sensing performance as shown in Figure 3B. Here, the sensing element is the top gate and to change the signal produced from the FET device a piezoresistive effect can be engaged. Subsequently, the cantilever's strain decreases the electron's mobility in the base, thus the leakage current is reduced.[54]
iii) Solution-gate configuration: This configuration setup offers a good ambiance with a straightforward process to observe/detect the physiological analytes of interest at low-gate operating potentials. Like an electrochemical cell, a miniaturized Ag/AgCl, Ag, and Pt reference electrode in the form of wire and needle is dipped in the solution chamber as a gate electrode, as depicted in Figure 3C[83] The FET device operates by applying gate-source voltage (V_{gs}) and drain–source voltage (V_{ds}) between the electrically conductive active channel/layer/materials including graphene, reduced graphene oxide (rGO), or other materials. Owing to the nanoelectric double layer, at the interface between the active material/layer and electrolyte solution superior sensitivity toward various biological analytes can be achieved.[42,47,53,54,56,81–86,99,100]

4. Critical Parameters for Assessment of Sensor toward High-Performance Analytics

The reliability, defined as consistent quantitative or qualitative analytical responses, needs to be validated to assess the usability of sensors. In clinical diagnostics, the important parameters for assessment include ultrahigh sensitivity, rapid detection/response time, selectivity, linearity, detection limit, reusability and reproducibility, interference-free detection, long-life span, etc. Recent trends emphasize the use of advanced nanoarchitectures to achieve the above-mentioned parameters. How these vital parameters influence the sensing performances of the FET devices is discussed in the following sections.

4.1. Sensitivity and Detection Limit (LOD)

The sensitivity mainly depends on the change in output current (drain current I_d) and field-effect mobility (μ_{FE}) when the active layer of the sensor's surface interacts with the target bioanalytes. Sensitivity is assessed by placing the target bioanalyte in contact with the sensor surface and measuring the change in the output current. Typically, this simple process involves three stages, i) the interaction/addition of the target analyte on top of the active layer of the sensor surface leads to a change in the concentration of the analyte, ii) interaction of the analyte with the receptor changes the density of bound charge, thereby resulting in a change in gate voltage that leads to iii) a change in output drain current signal. The mobility of charge carrier concentration in relationship with the output current can be also used to assess the sensitivity using Equation (2)

$$\mu_{FE} = g_m L / WCV_{ds} \tag{2}$$

where g_m, L, W, C, and V_{ds} are the differential transconductance, active channel length, active channel width, gating capacitance, and source–drain voltage.[87]

Next, the limit of detection or detection limit indicates the smallest solute quantity or concentration that can be recognized by the consistent reliability of the sensor output signal from the absence of that substance (control) (signal-to-noise ratio, SNR = 3). It is expressed in units of concentration.

4.2. Selectivity and Anti-Interference

Selectivity of the sensor is one of the most vital factors to be considered in the fabrication of FET sensor devices. The selectivity of the sensor crucially depends on the ability of the receptor to bind only the target bioanalytes of interest, resulting in minimal noise from other coexisting molecules present in the biological sample.[30,88–90] The selectivity and anti-interference can be simply assessed from a calibration curve for the coexisting interfering elements and equated to the targeted analyte calibration curve, as depicted in Figure 4C. Selectivity at this point is stated as the ratio of the output signal of the target analyte to the signal generated by interfering elements, at the same concentration of both samples.

4.3. Response Time

The response time of the biosensor is grouped into steady-state and transient response times. Steady-state response time is the time needed to achieve 95% of the steady-state response of the biosensor. It can be simply defined by the addition of each

analyte during the performance evaluation of the biosensor. Whereas transient response time is termed as the first derivative of the output signal to reach its highest value during the addition of the analyte. Both are dependent factors that rely upon the activity of the molecular detection system and the analyte (i.e., shorter response time due to higher activity and vice versa).

4.4. Linearity

The calculated response of the sensor's accuracy attributes to linearity. Mathematically, linearity can be represented as $y = mc$, where y is the output signal, c is the analyte concentration, and m is the biosensor's affectability. A small change in analyte concentration affects or makes a difference in the biosensor's output. The linear range with linearity is a considerable change in the output signal with respect to a small change in analyte concentrations is another important parameter to be considered. The linear calibration curve with regression coefficient can be obtained by plotting the different analyte concentrations along with their respective peak current responses attained for each analyte concentration.

4.5. Stability

The ability of biosensors to be stable or constant or a steady state in different environmental circumstances all around the biosensing structure. An error may occur due to any disturbance from the sensing system which may arise from the transducer, electronics, pH, temperature, buffer composition, analytes binding affinity toward bioreceptor, etc., which could influence the evaluation parameters and performance of the biosensor. Hence to achieve good efficiency the biosensor investigation demands high stability by maintaining the exact operational parameters and sensor structure.

4.6. Economical Commercialization

The early stage detection of various diseases including cancer, diabetes, physiological disorder, etc. shrinks the post-treatment cost heavily as well as facilitates good health through simple pre-treatment medications. In such a way, these FET sensors are more economical, furthermore, the alternative materials, substrates usages, and the engagement of facile and cost-effective process can lead to economical commercialization of the product.

4.7. Reproducible, Repeatable, Reusable/Disposable

Repeatability and reproducibility refer almost equivalent to each other, it is the results of consecutive experiments of the same concentration and performed in the different (reproducibility) or same (repeatability) situations associated with operating conditions (pH, temperature, etc.), process, same or different time interval analysis, etc.[91,92] Also, the fabricated FET device and the materials involved must be biocompatible/biodegradable, i.e., easily disposable in nature.

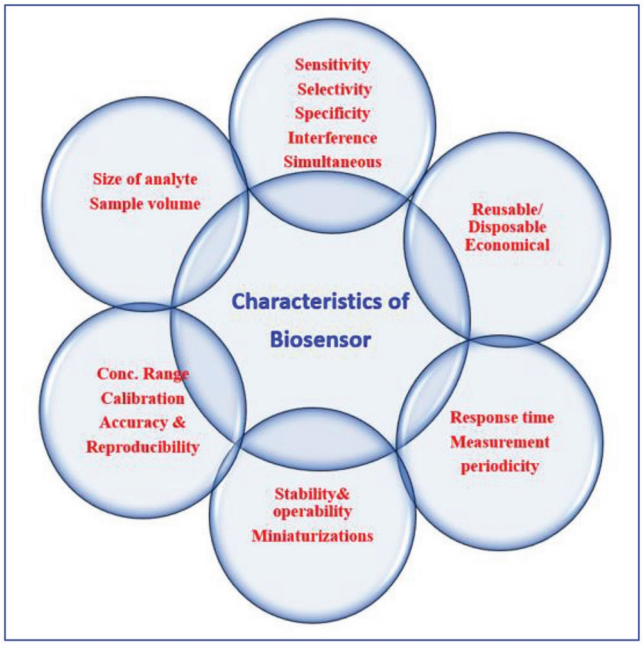

Figure 5. Biosensor characteristics.

Hence, all these mentioned vital factors as depicted in **Figure 5** need to be considered for designing and fabricating an efficient sensor device for realistic applications in highly sensitive clinical diagnostics, healthcare, pharmaceuticals, food, and agricultural industries.

5. Bioreceptors Involved in FET Biosensors

5.1. Functionalization of Active Surface with Biorecognition/Bioreceptor Element

The issue with nonspecific targeting or binding heavily affects the sensor performance. Bioreceptors are the molecules that facilitate specific interactions with the target bioanalyte/biomarker molecules. The bioreceptors play a vital role in target selectivity and specificity, i.e., the specific binding with the target analyte of interest by discriminating the coexisting molecules or substances in the complex biological samples, as depicted in **Figure 6**A. Not only the selectivity and specificity but also the sensitivity depends on the Debye screening length which is decided by the usage of size-dependent bioreceptors. The usage of target-specific biorecognition elements such as antibodies, aptamers, and complementary DNA along with the respective biomarkers (Figure 6B) is discussed in the following sections.

5.2. Antibodies

Antibodies are "Y"-shaped protective proteins secreted by B-lymphocytes and are an important part of the immune response in

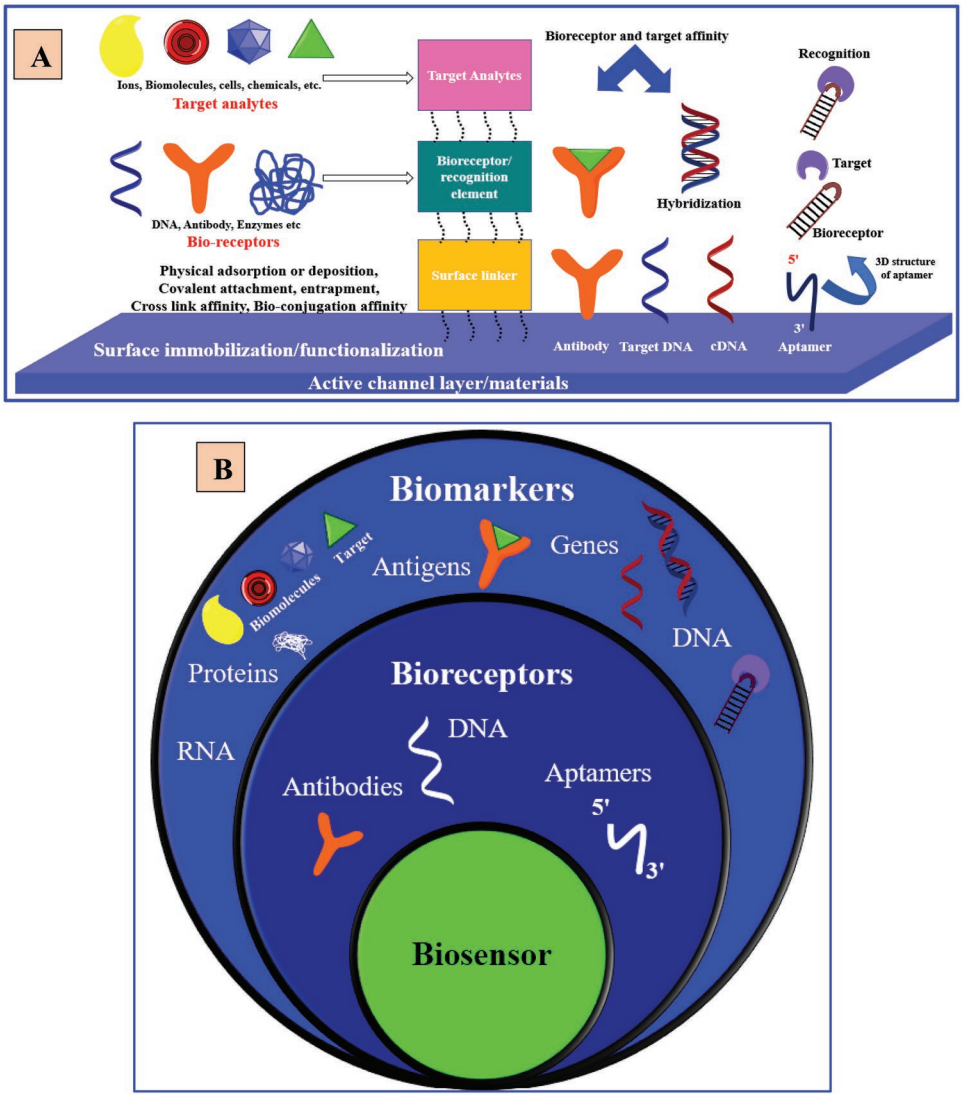

Figure 6. A) Mechanism and process of interactions between the bioreceptors and biomarkers. B) Biosensor with different bioreceptor and biomarkers.

mammals. Each type of antibody binds a specific antigen with very high selectivity, which makes it possible to use antibodies for the detection of target-specific analytes/antigens.[93–95] For example, genetically engineered antibodies functionalized by Pt nanoparticles (NPs) were used to decorate graphene transistors for the recognition of human epidermal growth factor receptor (HER3) biomarkers used for breast cancer detection.[93] In this study, a single-chain adjustable antibody fragment, capable of binding HER3 was used. The noticeable advantage is that the single-chain variable antibodies fragment is smaller (2–3 nm) than the conventional antibodies (10–15 nm). Likewise, Lerner et al.[95] made a single-chain variable antibody fragment by the modification of the 23C3 monoclonal antibody. An efficient diagnostic substitute to the Hu23C3 therapeutic antibody was noticed by employing the modified single-chain antibody fragment which holds the capability to stick with osteopontin. Also, the authors reported the antigen-specific concentration-dependent sensor response to OPN in the buffer. Based on this, the sensor could reliably differentiate between pure buffers and buffers containing atomic level concentrations of OPN, as depicted in **Figure 7**A. For the selective detection of cancer biomarkers, graphene encapsulated NP-based biosensor was fabricated. Here, the authors employed monoclonal antibodies against HER2 or epidermal growth factor receptor (EGFR) proteins.[96]

In terms of economy, an FET biosensor can be 20 times cheaper than the ELISA, as demonstrated by Sungkyung et al.,[97] using paper and multi walled carbon nanotubes as a substrate. The sensor surface was functionalized by prostate specific antigen antibody (PSA) antibody and the resistance changes in the PSA and PSA antigens binding levels are indirectly detected. Additionally, the sensitivity and detection range of the fabricated sensor make it suitable for early stage detection and diagnosis of prostate cancer (>4 ng mL^{-1} of PSA).

CD63 antibody was employed to achieve target-specific interaction with exosomes reported by Yu et al.,[98] shown in Figure 7B. Reduced graphene oxide (RGO) was used as the active sensor material. This FET device achieved a low detection limit of ≈33 particles μL^{-1}. Furthermore, the FET biosensor efficiently

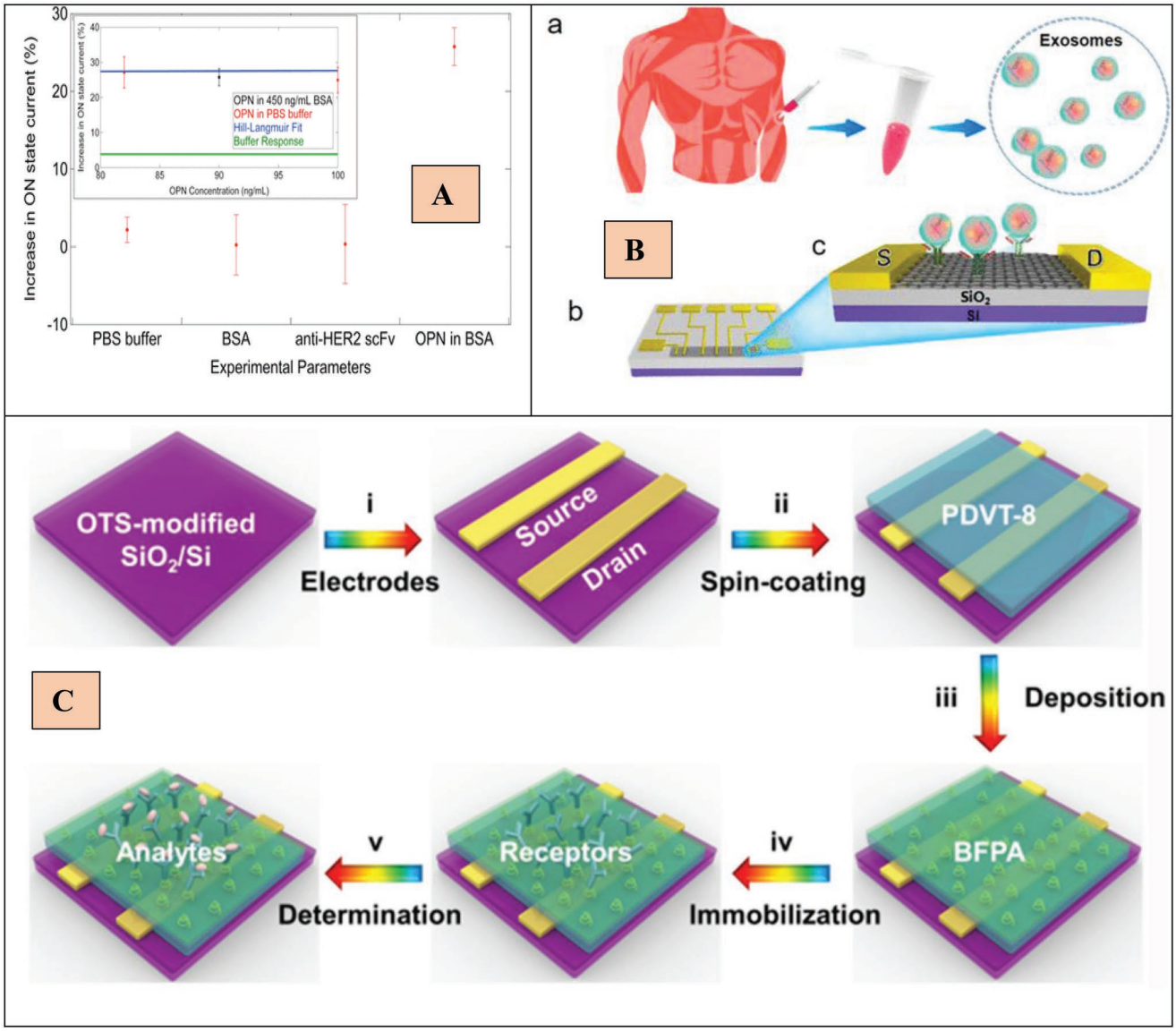

Figure 7. A) Devices exposed to neat phosphate buffer solution (PBS) buffer showed a response of +4%. Exposure to bovine serum albumin (BSA) at 450 ng mL^{-1} gave a null response. Devices prepared with the anti-HER2 scFv antibody in place of anti-OPN scFv and exposed to 90 ng mL^{-1} OPN also gave a null response. (Inset) Devices prepared with anti-OPN scFv antibodies and exposed to a mixture of 90 ng mL^{-1} OPN and 450 ng mL^{-1} BSA background protein gave a response identical to that expected for 90 ng mL^{-1} OPN in plain buffer. Reproduced with permission.[95] Copyright 2011, American Chemical Society. B) Schematic diagram of a CD63 antibody functionalized RGO FET biosensor for detection of exosomes. a) Exosomes are isolated and purified from the blood of patients. b) RGO FET biosensor. c) After anti-CD63 functionalization in the sensing region, exosomes can be directly bound to the CD63 antibody functionalized RGO FET biosensor for electrical and label-free detection. Reproduced with permission.[98] Copyright 2019, American Chemical Society. C) Fabrication of organic field effect transistor (OFET)-based biosensors. i) Au source and drain electrodes are deposited on OTS modified SiO_2/Si substrates, ii) PDVT-8 film is spin-coated as the charge transport layer, (iii) BFPA functional layer is modified on the device as the functional layer, iv,v) AFP antibodies are immobilized to form the receptor layer for the determination of target AFP biomarkers. Reproduced with permission.[99] Copyright 2021, American Chemical Society.

detected exosomes, that can be able to depict significant transformations in prostate cancer (PCa) patients and healthy people from their respective clinical serum samples, signifying it could be a promising tool for early stage cancer diagnosis.

Chenfang et al.[99] reported an ultrasensitive organic FET biosensor for early stage liver cancer detection by alpha-fetoprotein (AFP) based antibodies as depicted in Figure 7C. CYFRA21-1 and CYFRA21-1 polyclonal antibodies were engaged for the fabrication of a rapid, direct, highly sensitive, and target-specific biosensor.[100] Irrespective of advantages, it also possesses drawbacks, such as regeneration and reproducibility difficulties, complexity in the model generation, and lack of stability which limits its usage in some cases.

5.3. Aptamers

Aptamers are artificial single-stranded oligonucleotides with 15–40 nucleotides length, generally designed by a method called Systemic Evolution of Ligands by Exponential Enrichment

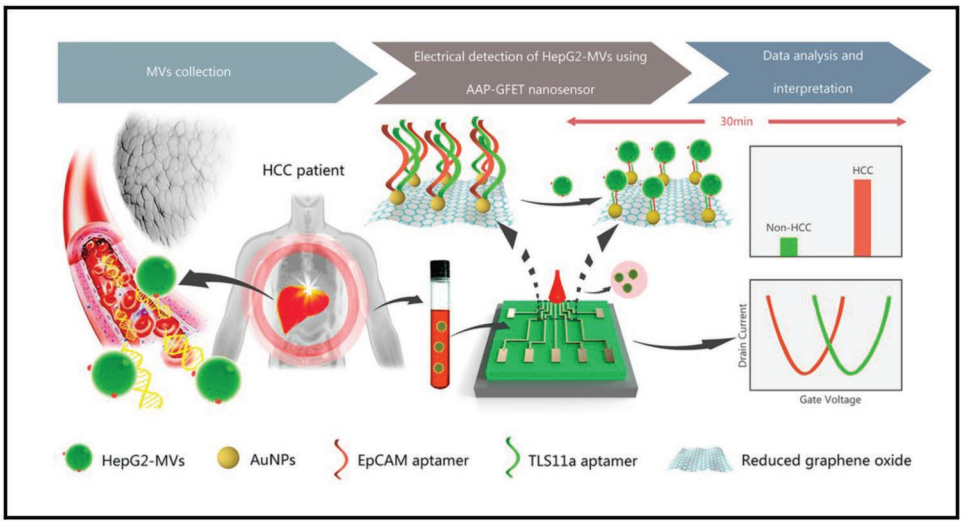

Figure 8. Three-step procedure for the electrical detection of hepatocellular carcinoma-derived MVs from blood samples using the AAP-GFET nanosensor. HCC, hepatocellular carcinoma. Reproduced with permission.[104] Copyright 2020, American Chemical Society.

(SELEX). In comparison with antibodies, aptamers are very small in size (around 1/10th of an antibody), have lower immunogenicity, and owing to their thermostability and tuneability, can be highly target-specific toward various analytes such as biomolecules, proteins (e.g., cytokines), and metal ions. Further, aptamers can be used for the delivery of drugs selectively to the cancer spot, where they help kill cancer cells.[13,27,87,101–103,106]

Ding et al.[104] reported a specific detection of hepatocellular carcinoma-derived microvesicles based on a dual-aptamer decorated graphene FET nanosensor, as depicted in **Figure 8**. For target-specific binding and HepG2-MVs detection, both epithelial cell adhesion molecule aptamer (AptEpCAM) and sulfhydrylated HepG2 cell-specific TLS11a aptamer (AptTLS11a) were attached to the surface of AuNP by an Au–S interaction. The fabricated nanosensor exhibited a wide linear output in the range from 6×10^5 to 6×10^9 particles mL^{-1} with a superior sensitivity of 84 particles μL^{-1} for HepG2-MVs detection.

Ziran et al.[105] developed a flexible, regenerative aptamer-based biosensor for wearable application using graphene–Nafion to detect and monitor Cytokine biomarkers in undiluted biofluids. The fabricated film facilitates the minimization of nonspecific adsorption and allows the biosensor's renewability. By means of these competencies, the sensor is proficient in sensitive and consistent monitoring cytokines in undiluted human sweat with an LOD down to 740 fM and a detection range from 0.015 to 250 nm. Guodong et al.[106] reported an aptamer-NP strip-based biosensor (ANSB) for highly sensitive cancer cell detection. Aptamers were carefully chosen from live cells by the cell-SELEX process and employed in the functionalization of ANSB for rapid, target-specific, highly sensitive, and economical sensing of circulating cancer cells.

5.4. DNA

FET-DNA biosensing typically involves a thermodynamic hybridization process, which requires designing DNA fragments that facilitate target-specific recognition of complementary target DNA (probe DNA or cDNA) via base pairing (hydrogen bonding between base pairs).[102,107–109]

Unnop et al. investigated molecular adsorption characteristics of methylated DNA on GO, as a possible basis for multicancer early stage detection.[110] Attomolar (aM) label-free DNA hybridization detection with electrolyte-gated graphene FET was studied by Rui et al.[111] The single nucleotide polymorphism (SNP) target specificity was accomplished by probing DNA immobilization over the surface of graphene via a pyrene-derived heterobifunctional linker. The graphene FET biosensor showed 24 mV dec^{-1} sensitivity with a detection limit of 25 aM as the lowermost concentration of target DNA for which the biosensor can be specific between an SNP-containing DNA and the perfect-match target sequence, shown in **Figure 9**.

A miniaturized, microfluidic system-based DNA-FET biosensor for quantification of two breast cancer biomarkers was reported by Huang et al. The fabricated DNA-FET biosensor detected 75 and 84 aM concentrations of microRNA-126 and microRNA-195, respectively.[112] Recently, a phosphorodiamidate morpholino oligos (PMO) altered graphene (G) G-FET sensor was developed for the coronavirus disease (COVID-19) identification. An amplification-free detection of Severe Acute Respiratory Syndrome (SARS)-CoV-2 RNAs was accomplished in this work by Li et al.[113] The developed sensor enables high sensitivity of SARS-CoV-2 RdRp with low background signal since PMO does not have charges. This method also resulted in a low LOD in PBS-0.37 fM, serum-3.99 fM, and throat swab-2.29 fM, a rapid response within 2 min was recorded for COVID-19 patients' samples. Zhang et al.[114] reported an ultrasensitive and direct miRNA detection using FET based on peptide nucleic acid (PNA)-immobilized silicon (Si) nanowires. The change in Si nanowires resistivity was recorded before and after hybridization between complementary miRNA targets and PNA probes. The detection limit was found to be 1 fM.

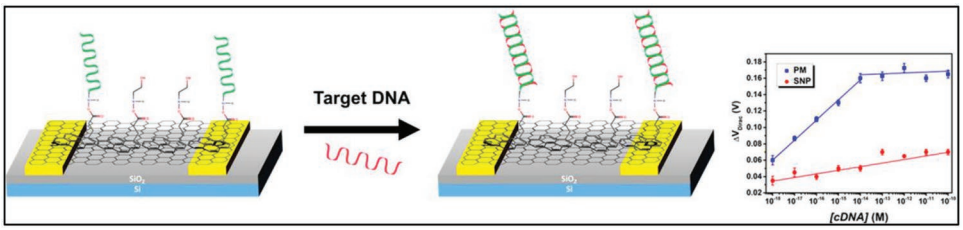

Figure 9. Attomolar label-free detection of DNA hybridization with electrolyte-gated graphene field-effect transistors. Reproduced with permission.[111] Copyright 2019, American Chemical Society.

6. Cancer Biomarkers Used for Diagnosis

6.1. Importance of Biomarkers in Detection and Pre-Treatment

Biomarkers are the biological molecules found in blood, other body fluids (cerebrospinal fluid, sweat, urine, saliva), and tissues that enable clinicians to differentiate between healthy individuals and cancer patients. Biomarkers exist also for other conditions, such as infections or metabolic diseases. Biomarkers can be different types of molecules, such as antibodies, nucleic acids (e.g., a microRNA or other non-coding RNA), peptides, proteins (e.g., an enzyme or bioreceptor), and others. Biomarkers are used to assess the patient's conditions in multistage clinical scrutiny, assessing the risk of any particular type of cancer, distinguishing the stages, and providing stratification of the malignancy type. Recently, many biomarkers were developed for noninvasive screening and early stage detection of cancer as well as in the prognosis of disease after treatment.[115,116] Thus, the biomarkers play a vital role in the patient follow-up and provide the basis for clinicians in their choice of interventions.

6.2. Antigens

An antigen is a substance (e.g., molecule, peptide, protein) that induces the body to create target-specific antibodies as an immune response. If an antigen is a cancer biomarker, the variation in the concentration of antigen is an indication that can help in identifying the stage of cancer.[119] For example, carcinoembryonic antigen (CEA) is a typical antigen biomarker for the stratification of lung, liver, and types of cancer. The most investigated CEA is a large cell surface acidic glycoprotein with a molecular weight of 200 kDa. Normal concentration of CEA in a healthy individual is from 2.5 to 5 ng mL^{-1}. Values above this threshold and their fluctuations can help in the diagnosis and prognosis of cancer.[117,120,121] Chenfang et al. reported a multibiomarker detection, using a simple functionalization approach, leading to ultrasensitive performance of organic protein biochips, as shown in **Figure 10**A. The fabricated biochip facilitates simultaneous detection of α-fetoprotein and CEA biomarkers with good reliability and enhanced sensitivity.[117,120,121] By employing a protein biomarker panel of CEA, squamous cell carcinoma (SCC) antigen, α1-antitrypsin, and retinol-binding protein, Patz et al. have succeeded in correctly classify 82% of healthy individuals and 88% of patients with lung cancer. The addition of biomarkers, such as CYFRA21-1, SCC, ENO1, and neuron-specific enolase, to a CEA-containing panel can further enhance the sensitivity of the device for the diagnosis of lung cancer.[117,120,121]

6.3. Genes

Genes are DNA-based inheritance units that transport hereditary characteristics to the child from parents. All cases of cancer are linked to gene mutations or changes in gene expression levels. Genetic cancer biomarkers (retinoic acid receptor-β mRNA, death-associated protein kinase, COX2, IL-8 mRNA, RASSFIA, etc.) can be used in DNA sequencing and arrays, polymerase chain reaction (PCR), reverse transcriptase PCR, fluorescent in situ hybridization, etc. to identify the genetic mutations or overexpression that takes place at the cancerous spot. These biomarkers are not only used in the detection of cancer but also in other diagnoses such as COVID-19.[118,122] In the case of lung cancer, the most common genetic abnormalities such as the promoter hypermethylation in tumor suppressor genes, loss of heterozygosity, and genomic instability are detected as microsatellite instability. Identifying the abnormalities via FET devices attracted attention owing to the target-specific binding and good sensitivity. Dong et al.[123] reported a multiprobe assay for detecting SEPT9 methylation by using carbon dot-decorated liquid-exfoliated graphene FET. The potential of this device to detect methylation is depicted in Figure 10B. The acquired hypermethylation in the promoter zone of the SEPT9 gene is linked with colorectal cancer (CRC) development. Moreover, superior sensitivity, allowing for detection of DNA samples of low quantity (2 ng) was achieved.

6.4. DNA

The blood circulation of cancer-affected patients carries tumor-linked DNA fragments. Hence, serum or plasma DNA can help to get predictive and prognostic information to plan for a pre-treatment assessment.[27] Bingjie et al. reported the fabrication of an rGO-based FET biosensor for ultrasensitive label-free PNA–DNA hybridization detection, as shown in Figure 10C.[124] Here, the detection of DNA was carried out via the hybridization of PNA–DNA by engaging rGO as the active material in this FET biosensor, with a limit of detection as low as 100 fM. Likewise, Chao et al.[125] reported an ultrasensitive FET DNA biosensor by a directional transfer method using chemical vapor deposition (CVD)-graphene as illustrated in

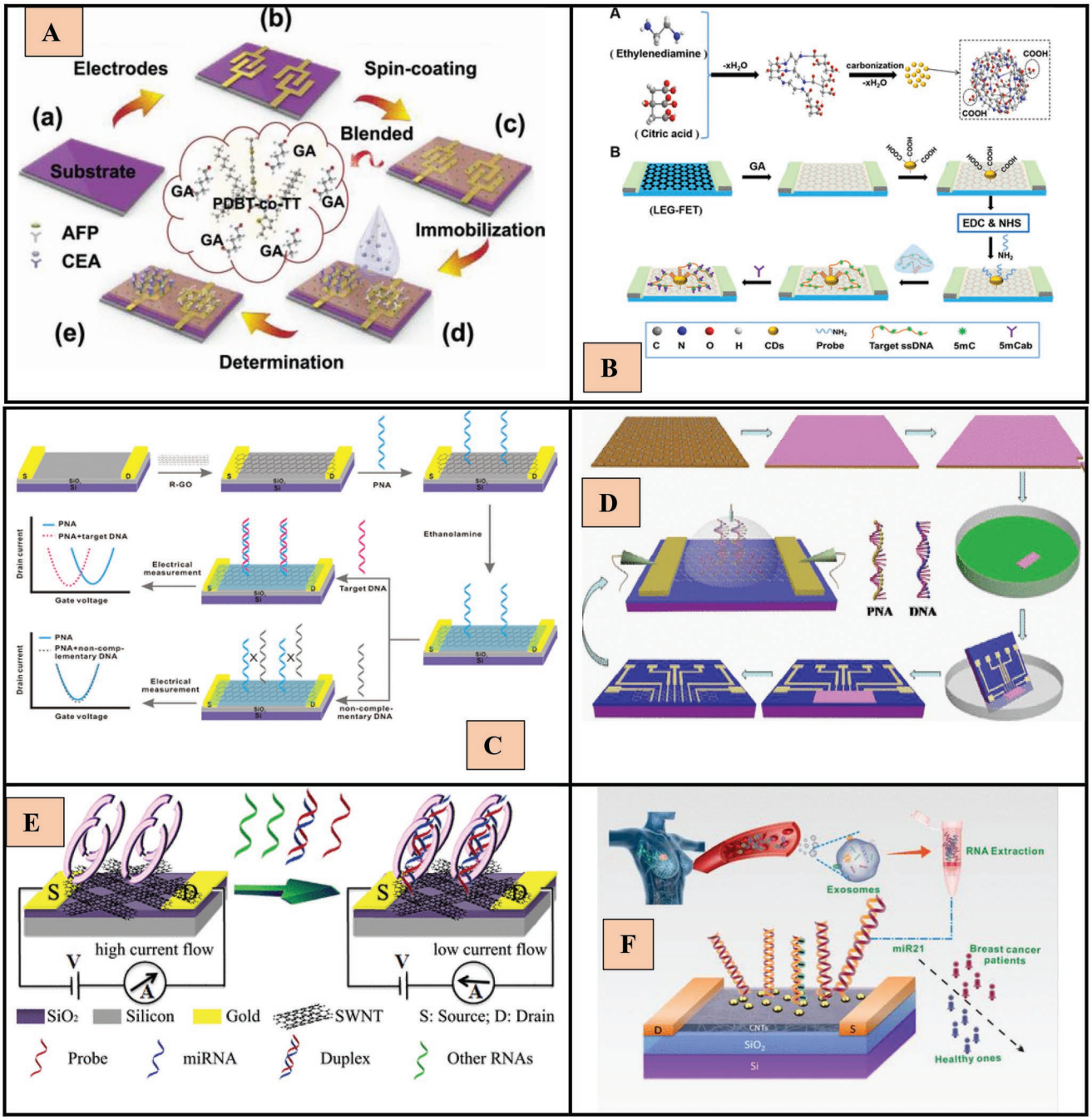

Figure 10. A) Schematic representation of OFET-based protein biochips. Reproduced with permission.[117] Copyright 2021, American Chemical Society. B) Protocol of the carbon dot (CD)-modified LEG-FETs and experimental design for the SEPT9 assay. Reproduced with permission.[123] Copyright 2020, American Chemical Society. C) Illustration of the R-GO FET biosensor for detection of DNA based on PNA–DNA hybridization. Reproduced with permission.[124] Copyright 2014, American Chemical Society. D) Table of content of fabrication of ultrasensitive field-effect transistor DNA biosensors by a directional transfer technique based on CVD-grown graphene. Reproduced with permission.[125] Copyright 2015, American Chemical Society. E) miRNA detection principle by the p-19 functionalized CNTs-FET nanobiosensor. Reproduced with permission.[129] Copyright 2013, American Chemical Society. F) Ultrasensitive detection of exosomal miR21 using the DNA-functionalized CNT FET biosensor. Reproduced with permission.[130] Copyright 2021, American Chemical Society.

Figure 10D. PNA was covalently immobilized on the graphene and the detection of DNA was achieved by subjecting target-specific DNA to the G-FET biosensor functionalized with PNA. The fabricated G-FET biosensor detected the target-specific DNA at a very low concentration of 10 fM.

6.5. Proteins

In cancer patients, there is abnormal secretion of proteins in the infected area. These proteins can be acquired from several sources such as blood, urine, sputum, and other body fluids.

Examples of abnormal secretions of proteins reported in cancer patients include D-Dimer, vascular endothelial growth factor, HER2 and 3, and EGFR, cytokine, dormant pancreatic stellate cells (pancreatic cancer), etc.[57,96,118,126,127] Tantipaiboonwong et al.[128] have reported urinary protein biomarkers and noticed that in lung cancer patients the urine test samples showed big differences at 14 and 28–42 kDa range. In this range, protein bands with higher intensity than in normal urine test samples were observed. Further, lung cancer patients' urine samples had low proteins at 50 kDa compared to the control samples. Also, they noticed that GM2 activator protein (GM2AP), transthyretin, CD59 glycoprotein, and Ig-free light chain showed differentially and could be employed as biomarkers for lung cancer detection.

6.6. RNA

For the regulation of genes, hematopoiesis, embryonic differentiation, and stratification of cancers, ribonucleic acid (RNA) and micro-RNA (miRNA) are vital. RNA-based biomarkers are widely employed in diagnostics. A target-specific, ultrasensitive, label-free, economical, point of care miRNAs detection device was developed by using a carbon nanotubes (CNT) FET, coupled to a Carnation Italian ringspot virus p19, as reported by Pankaj et al.[129] (shown in Figure 10E). Here, miRNA-122a was selected as the target material and first hybridized to a probe molecule. The fabricated biosensor showed a broad range up to 10^{-14} M with a low detection limit of 1 aM miRNA in the existence of a millionfold excess of total RNA. Likewise, a label-free, ultrasensitive, and stable FET biosensor through a polymer-sorted high-purity CNT film was fabricated for exosomal miRNA detection (depicted in Figure 10F).[130] Seongchan et al.[131] fabricated an electrical cartridge-based sensor that enables a reliable and straightforward determination of miRNAs in the urine of infected patients. The fabricated biosensor permitted a direct and rapid target-specific miRNAs detection in a wide dynamic range with a limit of detection down to 10 fM in human urine samples within 20 min while it also allows multiple miRNAs simultaneous quantification. Hence, based on the various research progressions RNA was engaged to monitor not only cancer but also it can be used for other disease diagnostic applications.

6.7. Other Types of Sensors and Materials in Cancer Detection

The wide variety of other numerous nanoarchitecture with radicals involved in the detection of cancer such as GO/rGO, MoS_2, NO, and indium phosphide nanowire (ZnO, and conducting polymers (e.g., polyaniline, polypyrrole (Ppy)). The employment of these various materials helped in achieving the detection by different modes of operations including colorimetric detection, fluorescence, surface plasmon resonance, electrochemical sensing process (including electrochemical impedance spectroscopy, amperometry, and differential voltammetry techniques), as well as FET, and so on.[98,132–144]

The performance of the FET biosensor toward the detection of various cancer biomarkers with their detection limit, sensitivity using various substrates, source and drain materials, and gate configurations were tabulated in the **Table 1**.

7. Factors to Improve the Performance of FET Biosensor toward Future Generation Diagnostic Devices Commercialization

The progress of future-generation electronic biosensor-based diagnostic devices with nanoengineered functionalities and advanced combinations into all types of substrates (from rigid (Si/SiO_2 wafers) to biodegradable, flexible, wearable substrates) will change the platform of real-time digital monitoring. In this perspective, reliable integration of advanced technologies to commercialize and improve the performance of FET-based biosensors opens various multidisciplinary applications including highly sensitive clinical diagnostics, healthcare, environmental monitoring of water and air quality, agriculture, health condition of animals, and plants, food and pharmaceuticals, etc. The following key parameters need to be highly spotlighted and explored to improve to reach the desired performance of the FET-based devices.

i) Device level: The device-level improvement includes suitable surface immobilization or functionalization of the active channel/materials of the sensor surface, no short channel effects, channel length modifications, and novel gate dielectric with innovative gate configurations as mentioned above. In the case of active channel length, the reduced channel length results in an increase in mobility as well as sensitivity but which affects the LOD.[27] Also, the reduced length results in less surface for functionalizing it with bioreceptor toward detection. Hence, the channel size needs to be optimized to the improvement of sensitivity as well as the limit of detection. Also, the most engaged low permittivity SiO_2 ($\varepsilon = 3.9$) dielectric layer with Si back gate needs an insecure operating gate voltage, i.e., 40–50 V.[57] In this work,[57] the conventional SiO_2 dielectric was replaced with HfO_2 ($\varepsilon = 16$) to run the device at a secured operating voltage as well as facilitates in desirable sensing environment. Further to improve, a hunt for an alternative substrate with a novel gate dielectric and gate configuration is required for the safe and efficient sensing performance of the future device.
ii) Measurement or operational level: The tunable measurement/operational techniques effectively enhance the device performance, thus grabbing the attention among the scientific community. The measurement strategies include gate bias optimization, signal amplification, and SNR reduction from the nontarget biomolecules, etc. and these improvements keep progressing toward the superior performance of the FET device. For example, the incorporation of advanced nanomaterials into the electrically active channel layer facilitates improving signal amplification through efficient charge transfer resulting in ultrahigh sensitivity.[13,27]
iii) Sensitivity and selectivity: Ultrahigh sensitivity and selectivity are vital properties to enhance the usage of the device. By proper surface immobilization/functionalization with target-specific bioreceptor/biorecognition element and also by

Table 1. FET biosensor-based detection of various cancer biomarkers.

Substrate used	Source/ Drain materials	Gate	Active layer/ transducer	Bioreceptors	Target	LOD	Sensitivity	Disease	Ref.
SiO_2/Si	Au/Cr	Back	Graphene	Aptamer	Cytokine IL-6	12 pM	–	Prostate, breast, and pancreatic cancer	[57]
SiO_2/Si	Ti/Pd	Back	Carbon nanotubes (CNT)	Single-chain variable fragment (scFv) protein	Osteopontin (OPN)	30 fM (1 pg mL^{-1})	–	Prostate cancer	[95]
SiO_2/Si	Au/Ti	Solution	Modified reduced graphene oxide decorated Au nanoparticles	TLS11a aptamer (AptTLS11a) and epithelial cell adhesion molecule aptamer (AptEpCAM)	HepG2 cell-derived microvesicles (HepG2-MVs)	–	84 particles μL^{-1}	Hepatocellular carcinoma	[104]
SiO_2/Si	Au	Back	Blended PDBT-co-TT/GA film	AFP and CEA	α-Fetoprotein and carcinoembryonic antigen	0.176 pM and 65 fM	–	Liver cancer	[117]
Glass	Ag	Solution	Carbon dot-modified liquid-exfoliated graphene	ssDNA	SEPT9	2 ng	–	Liver cancer	[123]
SiO_2/Si	Au/Ti	Solution	Reduced graphene oxide	Peptide nucleic acid (PNA)	DNA	10 fM	100 fM	Cancer	[124]
SiO_2/Si	Au/Ti	Solution	Single-layer graphene (SLG)	Peptide nucleic acid (PNA)	DNA	10 fM	10 fM	Cancer	[125]
SiO_2/Si	Au	Solution	Carbon nanotubes (CNT)	Carnation Italian ringspot virus p19 protein	MicroRNAs (miRNAs) -122a	1 aM	–	Cancer	[129]
SiO_2/Si	Au	Floating	Carbon nanotube (CNT)		Exosomal miRNA-21	0.87 aM	–	Breast cancer	[130]
ITO coated SnO_2	–	Solution	Reduced graphene oxide nanosheet	Peptide nucleic acid (PNA)	MiR21, miR1246	10 fM	–	Prostate cancer	[131]
Al_2O_3/Si	Au/Ti	Back	Molybdenum disulfide (MoS_2)	Antiprostate cancer antigen (anti-PSA)	Prostate cancer antigen (PSA)	100 fg mL^{-1}	–	Prostate cancer	[133]
SiO_2/Si	Ni/Au	Back	Silicon nanoribbon	–	Carcinoembryonic antigen (CEA)	10 pg mL^{-1}	–	Colorectal cancer	[149]
Poly(methyl methacrylate) (PMMA)	Au	Solution	Reduced graphene oxide nanosheets (rGO)	Anti-CA125 ssDNA	Carcinoma antigen (CA125)	5×10^{-10} U mL^{-1}	–	Ovarian cancer	[150]
SiO_2/Si	Polysilicon	Back	Magnetic graphene composite-modified polycrystalline-silicon nanowire	–	Apolipoprotein A II protein (APOA2 protein)	6.7 pg mL^{-1}	–	Bladder cancer	[151]
SiO_2/Si	Ti/Pt- $TiSi_2$	Solution	Organosilane self-assembled monolayer	–	1) Cytokeratin fragment 21-1 (CYFRA 21-1) and 2) neuron-specific enolase (NSE)	1) 1 ng mL^{-1} 2) 10 ng mL^{-1}	–	Lung cancer	[152]
SiO_2/Si	–	Solution	Glutaraldehyde modified surface	–	Alpha-fetoprotein (AFP)	10 ng mL^{-1}	–	Liver cancer	[153]

considering Debye screening, it is highly possible to achieve the atomic level detection of the desired bioanalyte or biomarkers toward cancer detection as well as other diseases. To overcome the Debye screening length limitations or increase the Debye screening length (Equation (3)), the following parameters need to be considered (shown in **Figure 11**): i) modifying the morphology of the active channel materials, ii) selection of appropriate or reducing the bioreceptor's size (e.g., cell (≈1 µm) > proteins (IgG ≈ 15 nm) > aptamers (few nm)), iii) choosing suitable functionalization/immobilization also electrolyte background with good ionic strength, and iv) device modulations.[145]

$$\lambda_D = \sqrt{\frac{\varepsilon_o \varepsilon_r K_B T}{2 N_a e^2 I}} \tag{3}$$

λ_D is the Debye screening length, ε_o and ε_r are gate dielectrics, K_B is the Boltzmann constant, T is the absolute

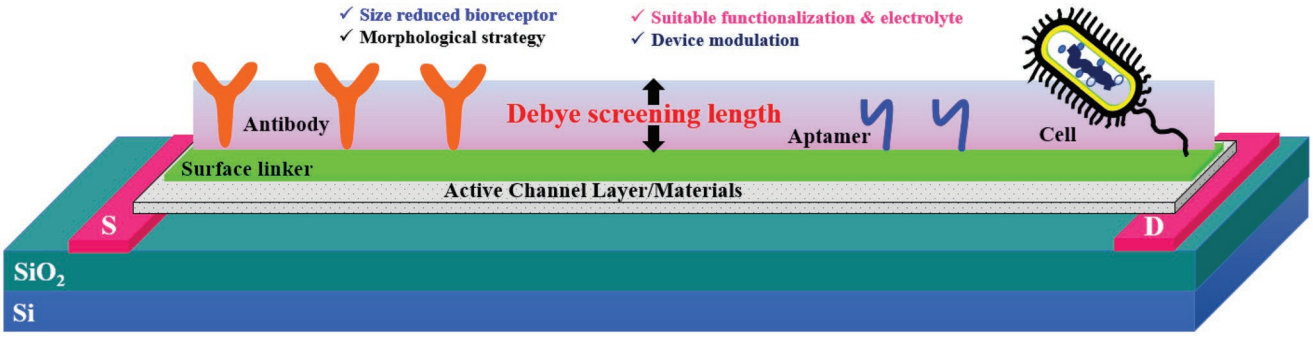

Figure 11. Strategies to overcome Debye screening length limitations.

temperature, N_a is the Avogadro's number, e is the elementary charge, and I is the ionic strength.

Also, to effectively use the sensor device for multipurpose analysis, simultaneous detection of multiple biomarkers with several distinctive multichannel sensing areas with different sensitive probes needs to be developed for improving the accuracy without compromising the sensitivity.[154,155]

iv) Reusable/disposable, long-term stability: The reproducibility and reliability of the sensors are limited, and poor regeneration leads to use it once only and throw the sensor. Hence the realistic demanding specifications need to be improved in the view of reproducibility, reusability, and reliability. To achieve and ensure much efficient regeneration, multiple experimentations need to be performed which include a) reproducibility check for the target-specific analyte several times, b) increasing the ionic strength of buffer solution, c) need to develop suitable reversible surface modification techniques (e.g., protein trapping systems),[146] and d) comparative analysis to ensure the linearity, stability, and compatibility of the fabricated device quantitative and qualitative analysis. For example, in the case of conductivity, the dielectric constant and its surface chemical properties regulate the capacitance effect between the electrically active conduction channel and the sensor surface which influences the conductivity of the device. The conventional device with SiO_2 as a dielectric interface offers undesirable low pH buffer capacity, leakage currents, drift, and hysteresis resulting in a nonlinear performance with unacceptable sensitivity, stability, and reproducibility. To improve all these essential parameters, materials with high-k offering higher transconductance and chemical stability need to be employed which facilitates refining the performances of sensitivity and linearity of the response to yield broader dynamic ranges as well as long-term stability.[57,154]

v) Commercialization of the diagnostic device: The thought-provoking void between the academic pioneering research concepts and commercialization is owing to the cost factor. The biosensor market growth is rising because of its unavoidable necessity and which is supported by the recent substantial technological developments in nanotechnology and nanoengineering. In 2021, the biosensors market is valued at $25.5 billion and is expected to reach $36.7 billion by 2026.[147] This estimation might reach a much higher level for the future direction of diagnostic devices and expands its commercialization, which needs much attention toward various factors which

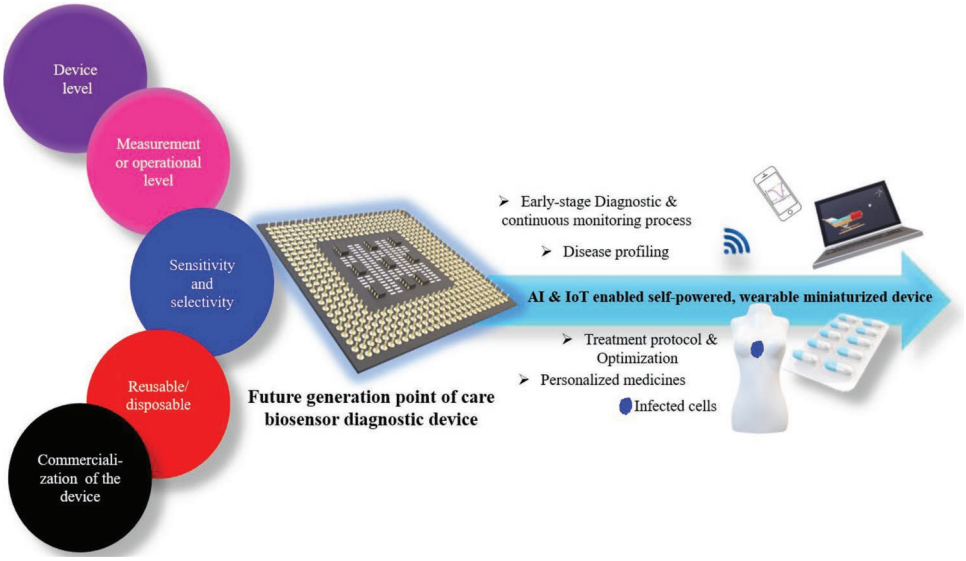

Figure 12. Future generation point of care biosensor-based diagnostic device integrated with multifunctional specifications.

include a) employment of organic materials (low-cost polymer materials, paper, etc.,)[148] and their combinations as active and substrate materials to achieve simplicity, flexibility, ease of processability, low power consumption, cost-effectiveness, b) reusable with large scale production, minimize the usage of additional reagents, operational conditions for the sensor devices, and c) Artificial intelligence and IoT integration with self-powered wearable/flexible/portable systems leads to continuous health care monitoring, as shown in **Figure 12**.

Ultimately all the highlighted points focus on the performance improvement and commercial viability of the sensor devices.

8. Conclusion with Current Challenges and Future Perspective

In conclusion, over the past decades, FET biosensor platforms attracted special attention leading to a drastic improvement in realistic applications. This review spotlights the roadmap to FET biosensors and emphasizes the important parameters to be considered during the design, fabrication, and assessing the sensing performances. Hence, it is vital to highlight those different parameters with the obstacles involved including design and multistep fabrication of FET device, surface activation with target-specific bioreceptor/recognition element, biomarkers identification toward specific diseases (Cancer, COVID-19, hepatitis B virus, influenza, etc.), the configuration of the device, measurement/operational conditions, which altogether aim toward highly selective, ultrasensitive biosensing performance. The electrical evaluation and performance of the FET biosensor devices with functionalization/immobilization with the target-specific bioreceptor activation toward biomarkers improved the sensitivity, selectivity, and allied properties. These advanced strategies and approaches can possibly augment their interdisciplinary applications in numerous fields such as highly sensitive clinical healthcare diagnostics, biomedical fields, food and pharmaceuticals, and agricultural fields.

With numerous research efforts, the focus of the field turns to the design and fabrications of future generation FET biosensors, mainly centered on wearable systems with artificial intelligence-based IoT integration, rapid and simultaneous detection of multiple biomarkers, self-powered, flexible, and portable with ultrahigh sensitivity with selectivity, reusable, reproducible, easily disposable, economical, etc. These fascinating features of FET devices facilitate providing complete information and continuous monitoring of human health is expected by the utilization of advanced materials with excellent conductivity, flexibility, long-term stability, etc. High-quality information acquired from the human via the advanced IoT integrated FET devices helps a lot in the early stage diagnosis of patients with not only cancer but also with other diseases (COVID-19, diabetes, etc.) paves a pathway to improve their health conditions by proper pre-treatment strategies with the respective medications. Hence, these various demanding specifications and features could open up novel opportunities for FET-based nanoelectronic devices in multidisciplinary applications in near future.

Acknowledgements

This work was supported by a grant from the Vinnova-Swelifes, Medtech4Healths [2020-04733], and Vetenskapsrådet.

Conflict of Interest

The authors declare no conflict of interest.

Keywords

biomarkers, bioreceptors, cancer detection, FET biosensors, sensitivity

Received: June 24, 2022
Published online:

[1] C. E. Meacham, S. J. Morrison, *Nature* **2013**, *501*, 328.
[2] R. Fisher, L. Pusztai, C. Swanton, *Br. J. Cancer* **2013**, *108*, 479.
[3] S. H. Hassanpour, M. Dehghani, *J. Cancer Res. Pract.* **2017**, *4*, 127.
[4] R. L. Siegel, K. D. Miller, A. Jemal, *CA-Cancer J. Clin.* **2018**, *68*, 7.
[5] A. Bhushan, A. Gonsalves, J. U. Menon, *Pharmaceutics* **2021**, *13*, 723.
[6] F. Vernia, M. Valvano, S. Fabiani, G. Stefanelli, S. Longo, A. Viscido, G. Latella, *Cancers* **2021**, *13*, 2361.
[7] M. Truong, B. Yang, D. F. Jarrard, *Urol. J.* **2013**, *189*, 422.
[8] C. Bax, G. Taverna, L. Eusebio, S. Sironi, F. Grizzi, G. Guazzoni, L. Capelli, *Cancers* **2018**, *10*, 123.
[9] K. E. Kaczor-Urbanowicz, F. Wei, S. L. Rao, J. Kim, H. Shin, J. Cheng, M. Tu, D. T. W. Wong, Y. Kim, *Biochim. Biophys. Acta, Rev. Cancer* **2019**, *1872*, 49.
[10] X. Wang, K. E. Kaczor-Urbanowicz, D. T. W. Wong, *Med. Oncol.* **2017**, *1*, 34.
[11] M. Al-Salhi, V. Masilamani, T. Vijmasi, H. Al-Nachawati, A. P. VijayaRaghavan, *J. Fluoresc.* **2011**, *21*, 637.
[12] Y. Ma, X. Wang, H. Jin, *Int. J. Mol. Sci.* **2013**, *14*, 10307.
[13] S. Mittal, H. Kaur, N. Gautam, A. K. Mantha, *Biosens. Bioelectron.* **2017**, *88*, 217.
[14] L. Wang, *Sensors* **2017**, *17*, 1572.
[15] K. E. Resnick, H. Alder, J. P. Hagan, D. L. Richardson, C. M. Croce, D. E. Cohn, *Gynecol. Oncol.* **2009**, *112*, 55.
[16] M. Y. Huang, H. L. Tsai, J. J. Huang, J. Y. Wang, *Transl. Oncol.* **2016**, *9*, 340.
[17] S. Mao, J. Chang, H. Pu, G. Lu, Q. He, H. Zhang, J. Chen, *Chem. Soc. Rev.* **2017**, *46*, 6872.
[18] L. Mu, Y. Chang, S. D. Sawtelle, M. Wipf, X. Duan, M. A. Reed, *IEEE Access* **2015**, *3*, 287.
[19] G. Hou, L. Zhang, V. Ng, Z. Wu, M. Schulz, *Nano LIFE* **2016**, *06*, 1642006.
[20] D. Bouilly, J. Hon, N. S. Daly, S. Trocchia, S. Vernick, J. Yu, S. Warren, Y. Wu, R. L. Gonzalez, K. L. Shepard, C. Nuckolls, *Nano Lett.* **2016**, *16*, 4679.
[21] J. Wang, F. Shen, Z. Wang, G. He, J. Qin, N. Cheng, M. Yao, L. Li, X. Guo, *Angew. Chem., Int. Ed.* **2014**, *53*, 5038.
[22] A. Noy, A. B. Artyukhin, N. Misra, *Mater. Today* **2009**, *12*, 22.
[23] P. Mehrotra, *J. Oral Biol. Craniofacial Res.* **2016**, *6*, 153.
[24] B. Shkodra, M. Petrelli, M. Aurora C. Angeli, D. Garoli, N. Nakatsuka, P. Lugli, L. Petti, *Appl. Phys. Rev.* **2021**, *8*, 041325.
[25] A. Béraud, M. Sauvage, C. M. Bazán, M. Tie, A. Bencherif, D. Bouilly, *Analyst* **2021**, *146*, 403.
[26] B. Chokkiah, M. Eswaran, S. M. Wabaidur, Z. A. Alothman, S. C. Lee, R. Dhanusuraman, *J. Mater. Sci.: Mater. Electron.* **2021**, *33*, 9245.

[27] I. Novodchuk, M. Bajcsy, M. Yavuz, *Carbon* **2021**, *172*, 431.
[28] M. Eswaran, P.-C. Tsai, M.-T. Wu, V. K. Ponnusamy, *J. Hazard. Mater.* **2021**, 126267.
[29] W. Tan, L. Sabet, Y. Li, T. Yu, P. R. Klokkevold, D. T. Wong, C.-M. Ho, *Biosens. Bioelectron.* **2008**, *24*, 266.
[30] E. Muthusankar, S. M. Wabaidur, Z. A. Alothman, M. R. Johan, V. K. Ponnusamy, D. Ragupathy, *Ionics* **2020**, *26*, 6341.
[31] P. M. Kosaka, V. Pini, J. J. Ruz, R. A. Da Silva, M. U. González, D. Ramos, M. Calleja, J. Tamayo, *Nat. Nanotechnol.* **2014**, *9*,1047.
[32] A. M. Vaidya, U. S. Annapure, *Food Biotechnol.* **2019**, *1*, 659.
[33] Q. Liu, C. Wu, H. Cai, N. Hu, J. Zhou, P. Wang, *Chem. Rev.* **2014**, *114*, 6423.
[34] S. Nakata, T. Arie, S. Akita, K. Takei, *ACS Sens.* **2017**, *2*, 443.
[35] S. Su, W. Wu, J. Gao, J. Lu, C. Fan, *J. Mater. Chem.* **2012**, *22*, 18101.
[36] Y. Cho, V. A. Pham Ba, J.-Y. Jeong, Y. Choi, S. Hong, *Sensors* **2020**, *20*, 3680.
[37] K. Melzer, V. D. Bhatt, E. Jaworska, R. Mittermeier, K. Maksymiuk, A. Michalska, P. Lugli, *Biosens. Bioelectron.* **2016**, *84*, 7.
[38] K. Maehashi, K. Matsumoto, Y. Takamura, E. Tamiya, *Electroanalysis* **2009**, *21*, 1285.
[39] J. P. Kim, B. Y. Lee, S. Hong, S. J. Sim, *Anal. Biochem.* **2008**, *381*, 193.
[40] J.-H. Jin, J. Kim, T. Jeon, S.-K. Shin, J.-R. Sohn, H. Yi, B. Y. Lee, *RSC Adv.* **2015**, *5*, 15728.
[41] P. Gou, N. D. Kraut, I. M. Feigel, H. Bai, G. J. Morgan, Y. Chen, Y. Tang, K. Bocan, J. Stachel, L. Berger, *Sci. Rep.* **2014**, *4*, 4468.
[42] K. Maehashi, T. Katsura, K. Kerman, Y. Takamura, K. Matsumoto, E. Tamiya, *Anal. Chem.* **2007**, *79*, 782.
[43] D. Cao, P. Pang, H. Liu, J. He, S. Lindsay, *Nanotechnology* **2012**, *23*, 085203.
[44] M. Pacios, I. Martin-Fernandez, X. Borrise, M. del Valle, J. Bartroli, E. Lora-Tamayo, P. Godignon, F. Perez-Murano, M. J. Esplandiu, *Nanoscale* **2012**, *4*, 5917.
[45] N. T. Tung, P. T. Tue, T. T. N. Lien, Y. Ohno, K. Maehashi, K. Matsumoto, K. Nishigaki, M. Biyani, Y. Takamura, *Sci. Rep.* **2017**, *7*, 1.
[46] I. Heller, A. M. Janssens, J. M€annik, E. D. Minot, S. G. Lemay, C. Dekker, *Nano Lett.* **2008**, *8*, 591.
[47] S. Rosenblatt, Y. Yaish, J. Park, J. Gore, V. Sazonova, P. L. McEuen, *Nano Lett.* **2002**, *2*, 869.
[48] C.-S. Lee, Y. Ju, J. Kim, T. H. Kim, *Sens. Actuators, B* **2018**, *275*, 367.
[49] S. Makarychev-Mikhailov, A. Shvarev, E. Bakker, *New Trends in Ion-Selective Electrodes, in Electrochemical Sensors, Biosensors and their Biomedical Applications*, Academic Press, San Diego, **2008**, p. 114.
[50] F. Khosravi, S. M. Loeian, B. Panchapakesan, *Biosensors* **2017**, *7*, 17.
[51] E. Stelmach, E. Jaworska, V. D. Bhatt, M. Becherer, P. Lugli, A. Michalska, K. Maksymiuk, *Electrochim. Acta* **2019**, *309*, 65.
[52] A. Palaniappan, W. Goh, D. Fam, G. Rajaseger, C. Chan, B. Hanson, S. Moochhala, S. Mhaisalkar, B. Liedberg, *Biosens. Bioelectron.* **2013**, *43*, 143.
[53] A. Palaniappan, W. Goh, J. Tey, I. Wijaya, S. Moochhala, B. Liedberg, S. Mhaisalkar, *Biosens. Bioelectron.* **2010**, *25*, 1989.
[54] F. Scuratti, G. E. Bonacchini, C. Bossio, J. M. Salazar-Rios, W. Talsma, M. A. Loi, M. R. Antognazza, M. Caironi, *ACS Appl. Mater. Interfaces* **2019**, *11*, 37966.
[55] S. Joshi, V. D. Bhatt, H. Wu, M. Becherer, P. Lugli, *IEEE Sens. J.* **2017**, *17*, 4315.
[56] G. Lee, J. Lim, J. Park, S. Choi, S. Hong, H. Park, *Curr. Appl. Phys.* **2009**, *9*, S25.
[57] Z. Hao, Y. Pan, W. Shao, Q. Lin, X. Zhao, *Biosens. Bioelectron.* **2019**, *134*, 16.
[58] L. Petti, N. Münzenrieder, C. Vogt, H. Faber, L. Büthe, G. Cantarella, F. Bottacchi, T. D. Anthopoulos, G. Tröster, *Appl. Phys. Rev.* **2016**, *3*, 021303.
[59] L. Petti, H. Faber, N. Münzenrieder, G. Cantarella, P. A. Patsalas, G. Tröster, T. D. Anthopoulos, *Appl. Phys. Lett.* **2015**, *106*, 092105.
[60] L. Petti, P. Aguirre, N. Münzenrieder, G. A. Salvatore, C. Zysset, A. Frutiger, L. Büthe, C. Vogt, G. Tröster, in *2013 IEEE Int. Electron Devices Meet.*, IEEE Xplore, Washington, DC, USA **2013**, p. 11.
[61] J. Jiang, J. Sun, W. Dou, Q. Wan, *IEEE Electron Device Lett.* **2011**, *33*, 65.
[62] P. F. Carcia, R. S. McLean, M. H. Reilly, *J. Soc. Inf. Disp.* **2005**, *13*, 547.
[63] G.-G. Lee, E. Tokumitsu, S.-M. Yoon, Y. Fujisaki, J.-W. Yoon, H. Ishiwara, *Appl. Phys. Lett.* **2011**, *99*, 012901.
[64] M.-J. Park, D.-J. Yun, M.-K. Ryu, J.-H. Yang, J.-E. Pi, O.-S. Kwon, G. H. Kim, C.-S. Hwang, J.-Y. Bak, S.-M. Yoon, *J. Mater. Chem. C* **2015**, *3*, 4779.
[65] S. H. Jin, S.-K. Kang, I.-T. Cho, S. Y. Han, H. U. Chung, D. J. Lee, J. Shin, *ACS Appl. Mater. Interfaces* **2015**, *7*, 8268.
[66] M. Nag, A. Chasin, M. Rockele, S. Steudel, K. Myny, A. Bhoolokam, A. Tripathi, *J. Soc. Inf. Disp.* **2013**, *21*, 129.
[67] J. Smith, A. Couture, D. Allee, *Electron. Lett.* **2014**, *50*, 105.
[68] T. Wadhera, D. Kakkar, G. Wadhwa, B. Raj, *J. Electron. Mater.* **2019**, *48*, 7635.
[69] A. A. Homaei, R. Sariri, F. Vianello, R. Stevanato, *J. Chem. Biol.* **2013**, *6*, 185.
[70] D. N. Tran, K. J. Balkus Jr., *ACS Catal.* **2011**, *1*, 956.
[71] C. S. Pundir, S. Lata, V. Narwal, *Biosens. Bioelectron.* **2018**, *117*, 373.
[72] A. Poghossian, M. J. Schöning, *Electroanalysis* **2014**, *26*, 1197.
[73] K. Liu, B. Ouyang, X. Guo, Y. Guo, Y Liu, *npj Flexible Electron.* **2022**, *6*, 1.
[74] Y. H. Lee, M. Jang, M. Y. Lee, O. Y. Kweon, J. H Oh, *Chem.* **2017**, *3*, 724.
[75] A. Sassolas, L. J. Blum, B. D. Leca-Bouvier, *Biotechnol. Adv.* **2012**, *30*, 489.
[76] J. Haccoun, B. Piro, V. Noel, M. C. Pham, *Bioelectrochemistry* **2006**, *68*, 218.
[77] S. Singh, P. R. Solanki, M. K. Pandey, B. D. Malhotra, *Sens. Actuators, B* **2006**, *115*, 534.
[78] B. Brena, P. González-Pombo, F. Batista-Viera. *Immobilization of Enzymes and Cells* (Ed: J. M. Guisan), Humana Press, Totowa, NJ **2013**, p. 15.
[79] A. Zhang, Y. Hou, N. Jaffrezic-Renault, J. Wan, A. Soldatkin, J.-M. Chovelon, *Bioelectrochemistry* **2002**, *56*, 157.
[80] J.-J. Xu, X.-L. Luo, H. -Y. Chen, *Front Biosci.* **2005**, *10*, 420.
[81] J. Oh, G. Yoo, Y. W. Chang, H. J. Kim, J. Jose, E. Kim, J. C. Pyun, K. H. Yoo, *Biosens. Bioelectron.* **2013**, *50*, 345.
[82] T. Chalklen, Q. Jing, S. Kar-Narayan, *Sensors* **2020**, *20*, 5605.
[83] D. Han, R. Chand, Y. S. Kim, *Biosens. Bioelectron.* **2017**, *93*, 220.
[84] H. Y. Zheng, O. A. Alsager, B. Zhu, J. Travas-Sejdic, J. M. Hodgkiss, N. O. Plank, *Nanoscale* **2016**, *8*, 13659.
[85] K. Melzer, V. D. Bhatt, T. Schuster, E. Jaworska, K. Maksymiuk, A. Michalska, P. Lugli, G. Scarpa, *IEEE Sens. J.* **2014**, *15*, 3127.
[86] K. Melzer, A. Münzer, E. Jaworska, K. Maksymiuk, A. Michalska, G. Scarpa, *Analyst* **2014**, *139*, 4947.
[87] L. Chao, Y. Liang, X. Hu, H. Shi, T. Xia, H. Zhang, H. Xia, *J. Phys. D: Appl. Phys.* **2022**, *55*, 153001.
[88] C. Bavatharani, E. Muthusankar, Z. A. Alothman, S. M. Wabaidur, V. K. Ponnusamy, D. Ragupathy, *Ceram. Int.* **2020**, *46*, 23276.
[89] E. Muthusankar, V. K. Ponnusamy, D. Ragupathy, *Synth. Met.* **2019**, *254*, 134.
[90] E. Muthusankar, D. Ragupathy, *Nano-Struct. Nano-Objects* **2019**, *20*, 100390.
[91] C. I. L. Justino, T. A. Rocha-Santos, A. C. Duarte, *Trends Anal. Chem.* **2010**, *29*, 1172.
[92] A. D. McNaught, *Compendium of Chemical Terminology*, Blackwell Science, Oxford **1997**, p. 1669.
[93] G. Z. Rajesh, R. Vishnubhotla, P. Ducos, M. D. Serrano, J. Ping, M. K. Robinson, A. T. C. Johnson, *Adv. Mater. Interfaces* **2016**, *3*, 1600124.
[94] J. Wu, T. Qiu, P. T. Pan, D. H. Yu, Z. G. Ju, X. W. Qu, X. Gao, C. B. Mao, L. Wang, *Asian Pac. J. Cancer Prev.* **2011**, *12*, 2921.

[95] M. B. Lerner, J. D'souza, T. Pazina, J. Dailey, B. R. Goldsmith, M. K. Robinson, A. T. C. Johnson, *ACS Nano* **2012**, *6*, 5143.
[96] A. K.-B. L. Sung Myung, A. Solanki, C. Kim, J. Park, K. S. Kim, *Adv. Mater.* **2011**, *23*, 2221.
[97] S. Ji, M. Lee, D. Kim, *Biosens. Bioelectron.* **2018**, *102*, 345.
[98] Y. Yu, Y.-T. Li, D. Jin, F. Yang, D. Wu, M. -M. Xiao, H. Zhang, Z.-Y. Zhang, G.-J. Zhang, *Anal. Chem.* **2019**, *91*, 10679.
[99] C. Sun, R. Li, Y. Song, X. Jiang, C. Zhang, S. Cheng, W. Hu, *Anal. Chem.* **2021**, *93*, 6188.
[100] N. Lu, A. Gao, P. Dai, H. Mao, X. Zuo, C. Fan, Y. Wang, T. Li, *Anal. Chem.* **2015**, *87*, 11203.
[101] Y. Wang, Y. Wang, X. L. Liu, L. J. Wu, L. H. Ding, C. Y. Effah, Y. J. Wu, Y. M. Xiong, L. L. He, *Biosens. Bioelectron.* **2022**, *195*, 113661.
[102] M. A. Morales, J. M. Halpern, *Bioconjugate Chem.* **2018**, *29*, 3231.
[103] L. S. Liu, F. Wang, Y. Ge, P. K. Lo, *ACS Appl. Mater. Interfaces* **2020**, *13*, 9329.
[104] D. Wu, Y. Yu, D. Jin, M. M. Xiao, Z. Y. Zhang, G. J. Zhang, *Anal. Chem.* **2020**, *92*, 4006.
[105] Z. Wang, Z. Hao, X. Wang, C. Huang, Q. Lin, X. Zhao, Y. Pan, *Adv. Funct. Mater.* **2021**, *31*, 2005958.
[106] G. Liu, X. Mao, J. A. Phillips, H. Xu, W. Tan, L. Zeng, *Anal. Chem.* **2009**, *81*, 10013.
[107] Y. H. Nien, T. Y. Su, J. C. Chou, P. Y. Kuo, C. H. Lai, C. S. Ho, Z. X. Dong, Z. X. Kang, T. Y. Lai, *IEEE J. Electron Devices Soc.* **2021**, *9*, 242.
[108] M. K. Anvarifard, Z. Ramezani, I. S. Amiri, *Mater. Sci. Eng., C* **2020**, *117*, 111293.
[109] Q. Zhang, H. S. Majumdar, M. Kaisti, A. Prabhu, A. Ivaska, R. Osterbacka, A. Rahman, K. Levon, *IEEE Trans. Electron Devices* **2015**, *62*, 1291.
[110] U. Srikulwong, W. Phanchai, P. Srepusharawoot, C. Sakonsinsiri, T. Puangmali, *J. Phys. Chem.* **2021**, *125*, 6697.
[111] R. Campos, J. Borme, J. R. Guerreiro, G. Machado Jr., M. F. Cerqueira, D. Y. Petrovykh, P. Alpuim, *ACS Sens.* **2019**, *4*, 286.
[112] C.-C. Huang, Y.-H. Kuo, Y.-S. Chen, P.-C. Huang, G.-B. Lee, *Microfluid. Nanofluid.* **2021**, *25*, 33.
[113] J. Li, D. Wu, Y. Yu, T. Li, K. Li, M.-M. Xiao, Y. Li, Z.-Y. Zhang, G.-J. Zhang, *Biosens. Bioelectron.* **2021**, *183*, 113206.
[114] G. J. hang, J. H. Chua, R. E. Chee, A. Agarwal, S. M. Wong, *Biosens. Bioelectron.* **2009**, *24*, 2504.
[115] N. L. Henry, Daniel F. Hayes, *Mol. Oncol.* **2012**, *6*, 140.
[116] L. Hartwell, D. Mankoff, A. Paulovich, S. Ramsey, E. Swisher, *Nat. Biotechnol.* **2006**, *24*, 905.
[117] C. Sun, M. V. Vinayak, S. Cheng, W. Hu, *Anal. Chem.* **2021**, *93*, 11305.
[118] S. K. Arya, S. Bhansali, *Chem. Rev.* **2011**, *111*, 6783.
[119] Z. Dai, J. Chen, F. Yan, H. Ju, *Cancer Detect. Prev.* **2005**, *29*, 233.
[120] F. Ye, M. Shi, Y. Huang, S. Zhao, *Clin. Chim. Acta* **2010**, *411*, 1058.
[121] E. F. Patz Jr., M. J. Campa, E. B. Gottlin, I. Kusmartseva, X. R. Guan, J. E. Herndon, *J. Clin. Oncol.* **2007**, *25*, 5578.
[122] A. Parihar, P. Ranjan, S. K. Sanghi, A. K. Srivastava, R. Khan, *ACS Appl. Bio Mater.* **2020**, *3*, 7326.
[123] D. Dong, J. Zhang, R. Zhang, F. Li, Y. Li, Y. Jia, *ACS Omega* **2020**, *5*, 16228.
[124] B. Cai, S. Wang, L. Huang, Y. Ning, Z. Zhang, G.-J. Zhang, *ACS Nano* **2014**, *8*, 2632.
[125] C. Zheng, L. Huang, H. Zhang, Z. Sun, Z. Zhang, G.-J. Zhang, *ACS Appl. Mater. Interfaces* **2015**, *7*, 16953.
[126] O. S. Kwon, S. J. Park, J. Y. Hong, A. R. Han, J. S. Lee, J. S. Lee, J. H. Oh, J. Jang, *ACS Nano* **2012**, *6*, 1486.
[127] Y. Shi, W. Gao, N. K. Lytle, P. Huang, X. Yuan, A. M. Dann, M. Ridinger-Saison, *Nature* **2019**, *569*, 131.
[128] P. Tantipaiboonwong, S. Sinchaikul, S. Sriyam, S. Phutrakul, S.-T. Chen, *Proteomics* **2005**, *5*, 1140.
[129] P. Ramnani, Y. Gao, M. Ozsoz, A. Mulchandani, *Anal. Chem.* **2013**, *85*, 8061.
[130] T. Li, Y. Liang, J. Li, Y. Yu, M.-M. Xiao, W. Ni, Z. Zhang, G.-J. Zhang, *Anal. Chem.* **2021**, *93*, 15501.
[131] S. Kim, S. Park, Y. S. Cho, Y. Kim, J. H. Tae, T. Il No, J. S. Shim, Y. Jeong, S. H. Kang, K. H. Lee, *ACS Sens.* **2020**, *6*, 833.
[132] R. Liu, X. Ye, T. Cui, *Research* **2020**, *2020*, 1.
[133] H. Park, G. Han, S. W. Lee, H. Lee, S. H. Jeong, M. Naqi, A. AlMutairi, *ACS Appl. Mater. Interfaces* **2017**, *9*, 43490.
[134] S. Barua, H. S. Dutta, S. Gogoi, R. Devi, R. Khan, *ACS Appl. Nano Mater.* **2017**, *1*, 2.
[135] O. N. Oliveira Jr., R. M. Iost, J. R. Siqueira Jr., F. N. Crespilho, L. Caseli, *ACS Appl. Mater. Interfaces* **2014**, *6*, 14745.
[136] L. Guo, Y. Shi, X. Liu, Z. Han, Z. Zhao, Y. Chen, W. Xie, X. Li, *Biosens. Bioelectron.* **2018**, *99*, 368.
[137] M. Xu, V. K. Yadavalli, *ACS Sens.* **2019**, *4*, 1040.
[138] M. A. Bangar, D. J. Shirale, W. Chen, N. V. Myung, A. Mulchandani, *Anal. Chem.* **2009**, *81*, 2168.
[139] Y. Park, M.-S. Hong, W.-H. Lee, J.-G. Kim, K. Kim, *Biosensors* **2021**, *11*, 114.
[140] S. C. Barman, M. Sharifuzzaman, M. Abu Zahed, C. Park, S. H. Yoon, S. Zhang, H. Kim, H. Yoon, J. Y. Park, *Biosens. Bioelectron.* **2021**, *186*, 113287.
[141] R. Janissen, P. K. Sahoo, C. A. Santos, A. M. Da Silva, A. A. G. Von Zuben, D. E. P. Souto, A. D. T. Costa, *Nano Lett.* **2017**, *17*, 5938.
[142] S. Ghosh, N. I. Khan, J. G. Tsavalas, E. Song, *Front. Bioeng. Biotechnol.* **2018**, *6*, 29.
[143] X. Zhan, S. Yang, G. Huang, L. Yang, Y. Zhang, H. Tian, F. Xie, C. M. Lamy de La, X. Yang, W. Fu, *Biosens. Bioelectron.* **2021**, *188*, 113314.
[144] F. Urabe, N. Kosaka, K. Ito, T. Kimura, S. Egawa, T. Ochiya, *Am. J. Physiol. Cell Physiol.* **2020**, *318*, C29.
[145] Z. Zheng, H. Zhang, T. Zhai, F. Xia, *Chin. J. Chem.* **2021**, *39*, 999.
[146] B.-R. Li, C.-C. Chen, U. R. Kumar, Y.-T. Chen, *Analyst* **2014**, *139*, 1589.
[147] A. Haleem, M. Javaid, R. P. Singh, R. Suman, S. Rab, *Sensors Int.* **2021**, *2*, 100100.
[148] V. Gubala, L. F. Harris, A. J. Ricco, M. X. Tan, D. E. Williams, *Anal. Chem.* **2012**, *84*, 487.
[149] Z. Bao, J. Sun, X. Zhao, Z. Li, S. Cui, Q. Meng, Y. Zhang, T. Wang, Y. Jiang, *Int. J. Nanomed.* **2017**, *12*, 4623.
[150] S. M. Majd, A. Salimi, *Anal. Chim. Acta* **2018**, *1000*, 273.
[151] H.-C. Chen, Y.-T. Chen, R.-Y. Tsai, M.-C. Chen, S.-L. Chen, M.-C. Xiao, C.-L. Chen, M.-Y. Hua, *Biosens. Bioelectron.* **2015**, *66*, 198.
[152] S. Cheng, S. Hideshima, S. Kuroiwa, T. Nakanishi, T. Osaka, *Sens. Actuators, B* **2015**, *212*, 329.
[153] S. Hideshima, R. Sato, S. Inoue, S. Kuroiwa, T. Osaka, *Sens. Actuators, B* **2012**, *161*, 146.
[154] S. Rollo, D. Rani, W. Olthuis, C. P. García, *Sens. Actuators, B* **2020**, *303*, 127215.
[155] C. Sun, G. Feng, Y. Song, S. Cheng, S. Lei, W. Hu, *Anal. Chem.* **2022**, *94*, 6615.

Muthusankar Eswaran is a postdoctoral researcher at the Department of Biology and Biological Engineering, Chalmers University of Technology, Sweden. He obtained his Ph.D. degree from the National Institute of Technology Puducherry, India. His area of expertise includes flexible, wearable nanoelectronics, nanotechnology, advanced materials-based FET and electrochemical sensors, supercapacitors, and fuel cells. His current research focuses on the fabrication of fully integrated self-powered nanoelectronic devices for highly sensitive healthcare diagnostics, and environmental monitoring.

Bavatharani Chokkiah is an assistant professor at the Department of Chemistry, Karpagam Academy of Higher Education, Coimbatore, India. She obtained her Ph.D. degree from the National Institute of Technology Puducherry, India. Her area of expertise includes nanotechnology, nanoelectrochemistry, analytical chemistry, flexible devices, advanced materials-based electrochemical sensor, supercapacitors, and fuel cells. Her current research focuses on the fabrication of fully integrated self-powered devices for healthcare diagnostics and environmental monitoring.

Santosh Pandit is a researcher at the Department of Biology and Biological Engineering, Chalmers University of Technology, Sweden. He obtained his Ph.D. degree from Chonbuk National University, Republic of Korea. His area of expertise includes bacterial biofilms, microbial resistant biomedical surfaces, and antimicrobial agents. His current research focuses on the antimicrobial coatings of graphene and other 2D materials on biomedical devices to prevent the device associated infections. His research also focuses to find novel antimicrobial/antibiofilm agents to prevent the biofilm associated infection as well as to reduce the possibility of antimicrobial resistance development.

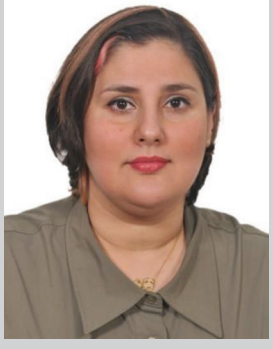

Shadi Rahimi is a researcher in Bacterial Systems Biology at the Chalmers University of Technology, Sweden. She obtained her Ph.D. in biotechnology from Kyung Hee University in South Korea. Her focus is on the bioapplication of graphene including sensor and drug delivery.

Ragupathy Dhanusuraman is an associate professor at the Department of Chemistry, National Institute of Technology Puducherry, India. He obtained his Ph.D. degree in chemistry from Kyungpook National University, Daegu, South Korea. His recent research includes nanotechnology for energy, catalytic and environmental applications.

Mahaboobbatcha Aleem is a postdoctoral fellow at the City College of New York, New York, USA. He obtained his Ph.D. degree from the PSG Institute of Advanced Studies, Coimbatore, India. His area of expertise includes the synthesis and fabrication of mono and multicrystalline silicon solar cells.

Ivan Mijakovic is a chaired professor of Bacterial Systems Biology at the Chalmers University of Technology, Sweden. He is also a professor and group leader at the Technical University of Denmark. He obtained his Ph.D. degree from the University Paris XI. He is an expert on bacterial protein phosphorylation and signaling and his group investigates the physiology of bacterial model organisms and pathogens. The Mijakovic group also develops metabolic engineering strategies and new approaches to fight bacterial infections: novel antibacterial agents, coatings, and graphene-based biosensors.